Int J Earth Sci (Geol Rundsch) (2015) 104:753–773
DOI 10.1007/s00531-014-1108-4

ORIGINAL PAPER

Syn-rift unconformities punctuating the lower–middle Cambrian transition in the Atlas Rift, Morocco

J. Javier Álvaro · Hassan Ezzouhairi · Sébastien Clausen · M. Luisa Ribeiro · Rita Solá

Received: 25 June 2014 / Accepted: 15 November 2014 / Published online: 28 November 2014

Abstract The Cambrian Tamdroust and Bab n'Ali Volcanic Complexes represent two magmatic episodes developed in the latest Ediacaran–Cambrian Atlas Rift of Morocco. Their rifting pulses were accompanied by accumulation of volcanosedimentary edifices (dominated by effusive lava flows in the former and explosive acidic aprons in the latter) associated with active tilting and uplift. Sealing of their peneplaned horst-and-graben palaeotopographies led to the onset of distinct onlapping geometries and angular discordances capping eroded basements ranging from the Ediacaran Ouarzazate Supergroup to the Cambrian Asrir Formation. Previous interpretations of these discordances as pull-apart or compressive events are revised here and reinterpreted in an extensional (rifting) context associated with active volcanism. The record of erosive unconformities, stratigraphic gaps, condensed beds and onlapping patterns across the traditional "lower–middle Cambrian" (or Cambrian Series 2–3) transition of the Atlas Rift must be taken into consideration for global chronostratigraphic correlation based on their trilobite content.

Keywords Tholeiitic volcanism · Uplift · Angular discordance · Palaeorelief · Condensation · Gondwana

J. J. Álvaro (✉)
Centro de Astrobiología (INTA/CSIC), Ctra. de Torrejón a Ajalvir km 4, 28850 Torrejón de Ardoz, Spain
e-mail: alvarobjj@cab.inta-csic.es

H. Ezzouhairi
Département de Géologie, Université Chouaib Doukkali, 24000 El Jadida, Morocco
e-mail: ezzouhairi_hassan@yahoo.fr

S. Clausen
Département de Géosciences, Université de Lille I, 59655 Villeneuve d'Ascq, France
e-mail: Sebastien.Clausen@univ-lille1.fr

M. L. Ribeiro · R. Solá
Laboratório Nacional de Energia e Geologia (LNEG), Ap 7586-Alfragide, 2610-999 Amadora, Portugal
e-mail: luisacarvalhoduarte@gmail.com

R. Solá
e-mail: rita.sola@lneg.pt

Introduction

Intracratonic rifts and their end products, passive-margin basins, are the expression of geological processes everlastingly shaping Earth's crust. Although sedimentary sequences contained within rift branches record the interplay between tectonics, volcanism and climate (Martins-Neto and Catuneanu 2010), the extent to which magmatism actively promotes extensional tectonics, and their related tilting and uplift processes, is poorly constrained. Normal faults, associated with volcanic centres and subsequent hydrothermal activity, contribute to the total strain budget across the rift and control sedimentary patterns, distribution of volcanic products and ore deposits of (sub)economic interest, and the onset of major stratigraphic discontinuities and angular discordances (Olsen and Morgan 2006; Corti 2012). Depending on the magnitude of uplift pulses, which can reach kilometre-scale elevations (McClay et al. 1998; Daradich et al. 2003), angular discordances may extend geographically from a few kilometres to hundreds of kilometres along rift branches. The latter are characteristic rifting features but, in some "fossil" rifts, such as the late Ediacaran–Cambrian Atlas Rift, they are still interpreted as the result of compressive events (see recent discussions in Álvaro and Clausen 2005; Landing et al. 2006; Landing and Geyer 2007; Álvaro 2014).

Relics of the Atlas Rift, which led to the Ordovician opening of the Rheic Ocean, occur throughout the Anti-Atlas, High Atlas, Jebilet, Rehamna and Coastal Meseta Ranges in Morocco. The rift was not a symmetric simple lineament, but was broken into distinct SSW–NNE-trending segments by transverse structures that propagated from SSW to NNE. Although a major syn-rift/post-rift transition related to fault-driven hydrothermal systems has been recently reported from the uppermost Ediacaran Taguedit Bed (Tabia Member of Adoudou Formation; Álvaro and Subías 2011; Álvaro 2013), subsequently overlain by the tectonically quiescent deposits of the Tifnout Member (Adoudou Formation), the rift still recorded renewed local tilting and uplift processes responsible for the record of lower and middle Cambrian discordances, such as those reported in the "lower Cambrian" Lemdad Formation (Álvaro and Clausen 2007) and marking the base of the "middle Cambrian" Brèche à Micmacca Member (Jbel Wawrmast Formation; Álvaro and Clausen 2006, 2008) and the Sidi-Saïd-Mâachou Volcanic Complex (Álvaro et al. 2008a). As a result, several syn-rift unconformities punctuated the stratigraphic record of the Atlas Rift, and a hierarchical statement of unconformities seems necessary to better understanding timing and spatial distribution of both angular discordances and erosive unconformities. This study is aimed at understanding the relationship between the tectonism, magmatism and sedimentation recorded in the Atlas Rift across the traditional "lower–middle Cambrian transition". This is crucial to properly applying global chronostratigraphic tools in a rifting sedimentary record punctuated by erosive unconformities, stratigraphic gaps, condensed beds and onlapping patterns.

Geological setting and stratigraphy

Relics of the latest Ediacaran–Cambrian Atlas Rift exposed in the Anti-Atlas and High Atlas are well-constrained chemo- and chronostratigraphically (see a recent synthesis in Álvaro et al. 2014a). The South Atlas fault (SAF in Fig. 1a) that longitudinally crosscut the High Atlas represents both (1) a palaeogeographical boundary that, during late Ediacaran–Cambrian times, separated a southern epeiric embayment (the so-called Souss Basin) and its northern basinal counterpart (Destombes et al. 1985; Álvaro et al. 2008a; Álvaro 2013) and (2) a Variscan major contact separating different styles of deformation (Soulaimani et al. 2014).

The traditional "lower–middle Cambrian" boundary interval lies across two distinct units: the Asrir and Jbel Wawrmast Formations (Fig. 2). The former (Choubert 1963), 30–80 m thick, is a weathering-resistant, heterolithic succession dominated by sandstones and shales with abundant volcanic ash interbeds, localized channel conglomerates and carbonate nodules and layers. Based on granulometric and colour features and geographical

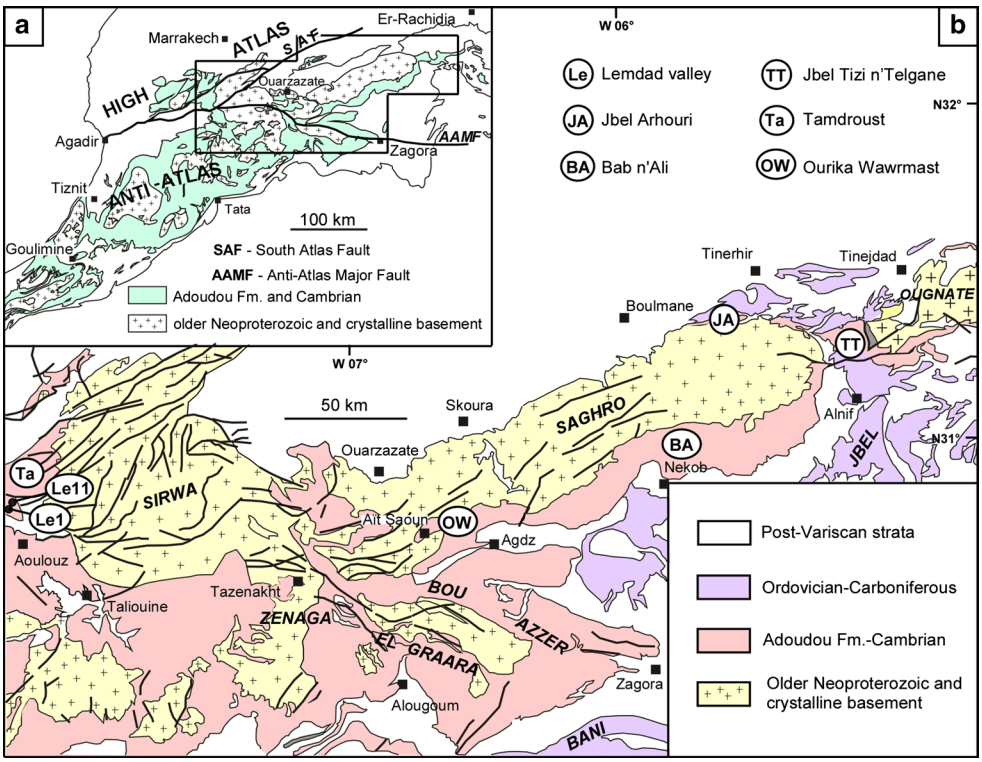

Fig. 1 Geological sketch of the Ouzellagh promontory (High Atlas) and Anti-Atlas (**a**) showing setting of the stratigraphic sections reported in the text (**b**); modified from Michard (1976)

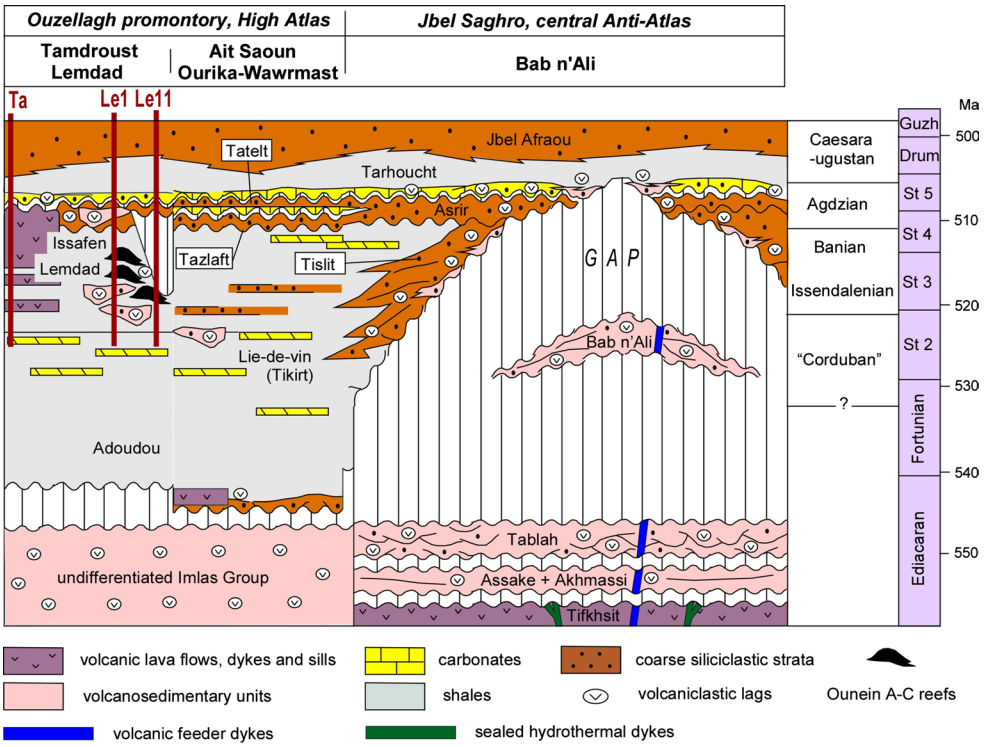

Fig. 2 Synthetized stratigraphic logs of the Tamdroust-Lemdad (High Atlas), Aït Saoun-Ourika Wawrmast (western margin of Saghro inlier) and Bab n'Ali Volcanic Complex (southern margin of Saghro inlier); data from Lemdad, Aït Saoun and Ourika Wawrmast after Álvaro and Clausen (2007, 2008) and Álvaro et al. (2008b); logs Le1 and Le11 detailed in Geyer and Landing (1995) and Álvaro and Clausen (2007) and Ta (Tamdroust) in this paper; global chronostratigraphic nomenclature after Gradstein et al. (2012) based on *ISCS* achievements; *Iss* Issafen Formation, *St* stage, *Drum* Drumian, *Guzh* Guzhangian, not at scale

distribution of facies, Geyer (1990) and Geyer and Landing (1995) subdivided Choubert's unit into four formations, which have recently been assigned to members of the Asrir Formation (Álvaro et al. 2014a). In the central Anti-Atlas (Fig. 1b), Landing et al. (2006) also subdivided the Asrir Formation into two formations (members in this paper), the Tazlaft and Tatelt Members, whose respective contacts were reported as erosive unconformities. The overlying Jbel Wawrmast Formation (Destombes et al. 1985), which is up to 300 m thick, can be subdivided into the Brèche à Micmacca and Tarhoucht Members. The former, up to 60 m thick, consists of variegated volcano-bioclastic limestones, shales and subsidiary conglomerates. K-bentonites, lava flows and volcanosedimentary aprons form the base of the member in some areas; two of them are detailed below. The 100- to 300-m-thick Tarhoucht Member is a coarsening-upward shale-dominated unit punctuated by whitish bioclastic limestones and ash levels, locally giving a variegated aspect to the host shale.

From a chronostratigraphic point of view, a global Cambrian Series 2/3 boundary has not yet been selected by the International Subcommission on Cambrian Stratigraphy (ISCS), and the use of the traditional "lower–middle Cambrian boundary" in the Western Mediterranean region of Gondwana is still a matter of dispute. In the Acado-Baltic biogeographical Province (Sdzuy 1972), which comprises Avalonia, the Mediterranean region and Baltica, the boundary has been traditionally taken at the basal olenellid-free strata bearing paradoxidine trilobites (Brögger 1879, 1886). However, this sketch was ruled out in Morocco, where Hupé (1953) pointed out a co-occurrence of olenellids and paradoxidids. A part of Hupé's (1960) "Aguilizian" and Choubert's (1963) "Ouriken n'Ourmast horizon" (the above-reported Brèche à Micmacca Member) was marked by a stratigraphic level, 50–60 m thick, with olenellids, protolenids and paradoxidids, resting in slight angular discordance on the substrate. The first occurrence of the Paradoxidinae is clearly diachronous throughout the Acado-Baltic Province and Siberia so Brögger's sketch cannot be maintained. At present, there are two regional trilobite-based proposals in the Western Mediterranean region. For Morocco, Hupé (1953, 1960) suggested as the base of the traditional "middle Cambrian" (Acadian) the oldest co-occurrence of olenellids, protolenids and paradoxidids. However, Geyer (1990) disagreed and suggested another boundary below this fossiliferous mélange, marked by the first appearance of the trilobite genus *Hupeolenus* (*H. hupei*, *H. termierelloides* or *H. dimarginatus*, the former endemic and the two latter also found in Spain). For the Iberian Peninsula, the series boundary is marked at the first appearance of the trilobite *Acadoparadoxides mureroensis* (Álvaro et al. 1993; Liñán et al. 1993), a taxon tentatively reported in Poland (Żylińska and Masiak 2007), Turkey (Dean 2005), Sardinia (Loi et al. 1995) and Morocco (Sdzuy 1995; Geyer and Vincent 2014). As both *A. mureroensis* and *Hupeolenus* species occur in the Iberian Peninsula and Morocco, their respective first occurrences can be used for regional

correlation before a formal Cambrian Series 2/3 boundary is officially selected by the ISCS.

Previous geodynamic interpretations

One of the most important rift-related volcanic episodes recorded in the Atlas Rift took place across the "lower–middle Cambrian transition". It is associated with the onset of the variegated, volcano-bioclastic limestones that characterize the Brèche à Micmacca Member and its basal discontinuity (Fig. 2). Coeval tectonic and volcanic factors were considered by Hupé (1955) to explain the occurrence of a low-angle discordance at the base of the Brèche à Micmacca Member in the Ouriken n'Ourmast region of the Jbel Saghro (Fig. 1b). He associated the setting of this anomalous contact with a supposed Salairian compression, by comparison with the homonymous Siberian orogeny. Subsequently, Boudda et al. (1975, 1979), Michard (1976) and Destombes et al. (1985) described this contact (Assirian/Ourmastian or lower–middle Cambrian boundary sensu Hupé 1953) as a mappable, low-angle discordance and gap counterpart, which was explained as the result of widespread uplift and subaerial exposure and fall in sediment input (with subsequent condensation). They interpreted the end of the traditional "early Cambrian" as an interval of high volcanic activity and tectonic instability, led by "epeirogenic" movements that were followed by widespread transgression on an inherited palaeorelief. As a result, a palaeorelief made up by the Ediacaran Ouarzazate Supergroup is directly onlapped by the Brèche à Micmacca in the northern Jbel Saghro (e.g. the Jbel Arhouri), the Jbel Ougnate and part of the High Atlas (Fig. 1b). Geyer and Landing (1995) also considered the Brèche à Micmacca as representative of an interval of basin reorganization, which featured the development of local volcanic flows, deposition of common K-bentonites and onlap across the Pan-African orogen. The authors considered this summary of geodynamic events as "epeirogenic" and not eustatic in origin.

Álvaro and Clausen (2005, 2006, 2008) reinterpreted the volcano-bioclastic limestone beds of the Brèche à Micmacca as hiatal shell accumulations due to their microstratigraphic subdivision by hiatal discontinuities coated by microbial crusts. They also recognized the presence of local microkarst structures controlled by dissolution, partial occlusion by sediment infill and, in some cases, by colonization of cryptic cavities by microbial mats and branching (putative algal) filaments. A rifting pulse of synsedimentary tilting, uplift and volcanism, with local emersion of palaeohigh shoulders, should represent a proper context for this scenario (e.g. Bernardin et al. 1988; Soulaimani et al. 2003; Pouclet et al. 2007; Álvaro et al. 2008a). The presence of archaeocyathan debris in the Brèche à Micmacca limestones (Buggisch et al. 1978; Álvaro and Clausen 2008) and heterolithic clasts and fossil skeletons exhibiting different diagenetic processes (Álvaro and Clausen 2006, 2008) allowed interpretation of these strata as condensed levels bearing fossils and lithoclasts reworked from older strata and overlaying stratigraphic gaps of variable time spans (Álvaro 2014) (Fig. 2).

Recently, Landing et al. (2006) and Landing and Geyer (2007) have suggested another geodynamic scenario in the central Anti-Atlas. They recognized two distinct unconformities, marking the Tazlaft/Tatelt (members of the Asrir Formation) and Tatelt/Brèche à Micmacca contacts, and interpreted them as reactivation pulses of a pull-apart or transtensional regime. The latter contact (the above-reported angular discordance) was supported by arguments such as the presence of local gentle folding and synsedimentary slumps. However, these were neither illustrated nor described, and the presence of slumps and olistostromes is a conspicuous feature in the vicinity of palaeoreliefs in the Anti-Atlas (Buggisch and Heinitz 1984; Álvaro et al. 2008b). In any case, this hypothesis is in need of description and quantification of prominent features of strike-slip faults with en-echelon fault and fold structures and microstructures. Until present, the presence of embedded volcanic and volcanosedimentary episodes in the central Anti-Atlas and southern High Atlas, punctuating the "lower–middle Cambrian boundary" interval, has been reported by Moussu (1959), Destombes et al. (1985) and Landing et al. (2006), but neither the geochemical affinity of their volcanic counterparts nor their relationship to distinct erosive unconformities was analysed in detail. A complete revision of the relationship between volcanism and sedimentary body geometries is characterized below in order to solve this puzzle of suggested geodynamic scenarios.

Explanatory note

The term epeirogenic is written above between quotation marks due to what we consider a semantic problem. "Epeirogenic" was coined by Gilbert (1890) to refer to "a form of diastrofism that has produced the larger features of the continents and oceans, for example, plateaux and basins, in contrast to the most localized process of orogeny, which has produced mountain chains" (for a synthesis, see Miall 2000). Modern studies of the thermal evolution of the mantle, supported by numerical modelling experiments, have provided a mechanism that explains the long-term uplift, subsidence and tilting of continental areas, especially large cratonic interiors beyond the reach of the flexural effects of plate-margins extension or loading (Burgess and Gurnis 1995; Burgess et al. 1997). Gurnis (1988, 1990) developed

the concept of dynamic topography, in which the Earth's elevation and that of oceans are related to the thermal properties of the mantle. The heat that accumulates beneath supercontinents can generate continental-scale upward of up to 1 km over time spans of 100 m.y. This process is the explanation for epeirogeny, broadly associated with vertical motions of the crust unrelated to plate-margins developed over long periods (several tens of m.y.) and broad upward and downward movements of several hundreds of metres. In contrast, rift zones evolve along pre-existing lineaments of the crust and may display initial thermally induced up-doming. As a result, uplifted and often tilted blocks neighbouring grabens and half-grabens represent shorter-term processes than epeirogenic vertical movements and affect regional (not continental) areas (Bennett et al. 2009; Saleeby et al. 2013). Therefore, the term "epeirogeny" (bearing a genetic meaning) seems inadequate to be used for describing local or regional uplifts (a descriptive term) in rifting areas, as has been currently recorded in the Atlas Rift case study.

Tamdroust Volcanic Complex

The Tamdroust Volcanic Complex crops out along the NNW–SSE-trending Jbel Ouchden (High Atlas), linking the villages of Tamdroust, Ait Yassine and Tiguicht (Fig. 3a). The complex comprises an area of c. 18 km^2 and consists of a succession of compound lava flows interbedded with dolostones, limestones, litharenites, conglomerates and variegated shales of the Lemdad and Issafen Formations (Fig. 4a). The Asrir Formation does not crop out in the study section, but is referred to laterally (Moussu 1959). An intrusion of Variscan ophites separates exposures of the Lemdad/Issafen Formations and the Tarhoucht Member. Emplacement of the complex was contemporaneous with sedimentation of the Issendalenian–lower Agdzian Lemdad, Issafen and Asrir Formations (sensu Geyer and Landing 1995, 2004). The presence of their derived volcaniclastic counterparts is evidenced by the wealth in pyroclastic interbeds punctuating these formations in the neighbouring Lemdad valley, located c. 9–10 km to the South (Boudda et al. 1975; Álvaro and Clausen 2007).

The Lemdad Formation, 240 m thick in the study area, consists of limestone, dolostone and variegated shale interbedded with lava flows and volcanosedimentary channels and beds. Thin-bedded carbonates commonly exhibit scouring bases, symmetric ripples, low-angle and parallel laminae and bioclastic (rich in echinoderm, trilobite and calcite-walled brachiopod debris) and stromatolitic fabrics. Close to lava flows, they are currently partly-to-wholly silicified (Fig. 4b) and display secondary dissolution processes with vug pores occluded with haematite (Fig. 4c). Interbedded, metre- to centimetre-thick, disrupted, faulted or slumped, disharmonic folds along with slump scarps and inclined slide planes are conspicuous and clearly bounded by undisturbed planar strata (Fig. 4d, e). Carbonate/shale interbeds are arranged in thickening-upward parasequences, up to 16 m thick, reflecting shallowing and prograding patterns from clayey offshore to peritidal stromatolitic build-ups (Fig. 4h), episodically punctuated by slumping processes. The Issafen Formation, 30 m thick in the study area, consists of monotonous shales punctuated by centimetre-thick grading litharenites, interpreted as tempestites in an offshore-dominated environment.

At least, four volcanic pulses associated with polyphase feeder dykes can be recognized embedded in the heterolithic strata of the Lemdad and Issafen Formations (Fig. 4a). Lava flows make up almost 40 % in thickness of both formations. Simple, non-pillowed and subsidiary pillowed, lava flows are 5- to 30-m-thick units, which display rough or undulating lower and upper surfaces. Their central

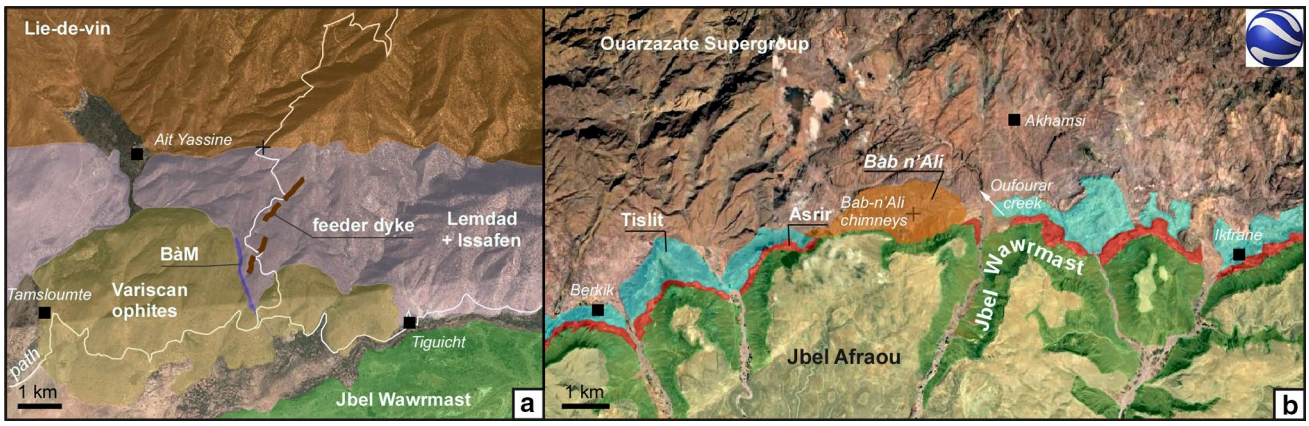

Fig. 3 Geological sketch of the Tamdroust (**a**) and Bab n'Ali (**b**) Volcanic Complexes on Google Earth images; GPS coordinates (*blue crosses*) for base of Lemdad Formation in **a** N30°54′08.63″ W08°07′56.39″ and Bab n'Ali chimneys in **b** N31°02′58.33″ W05°48′59.14″

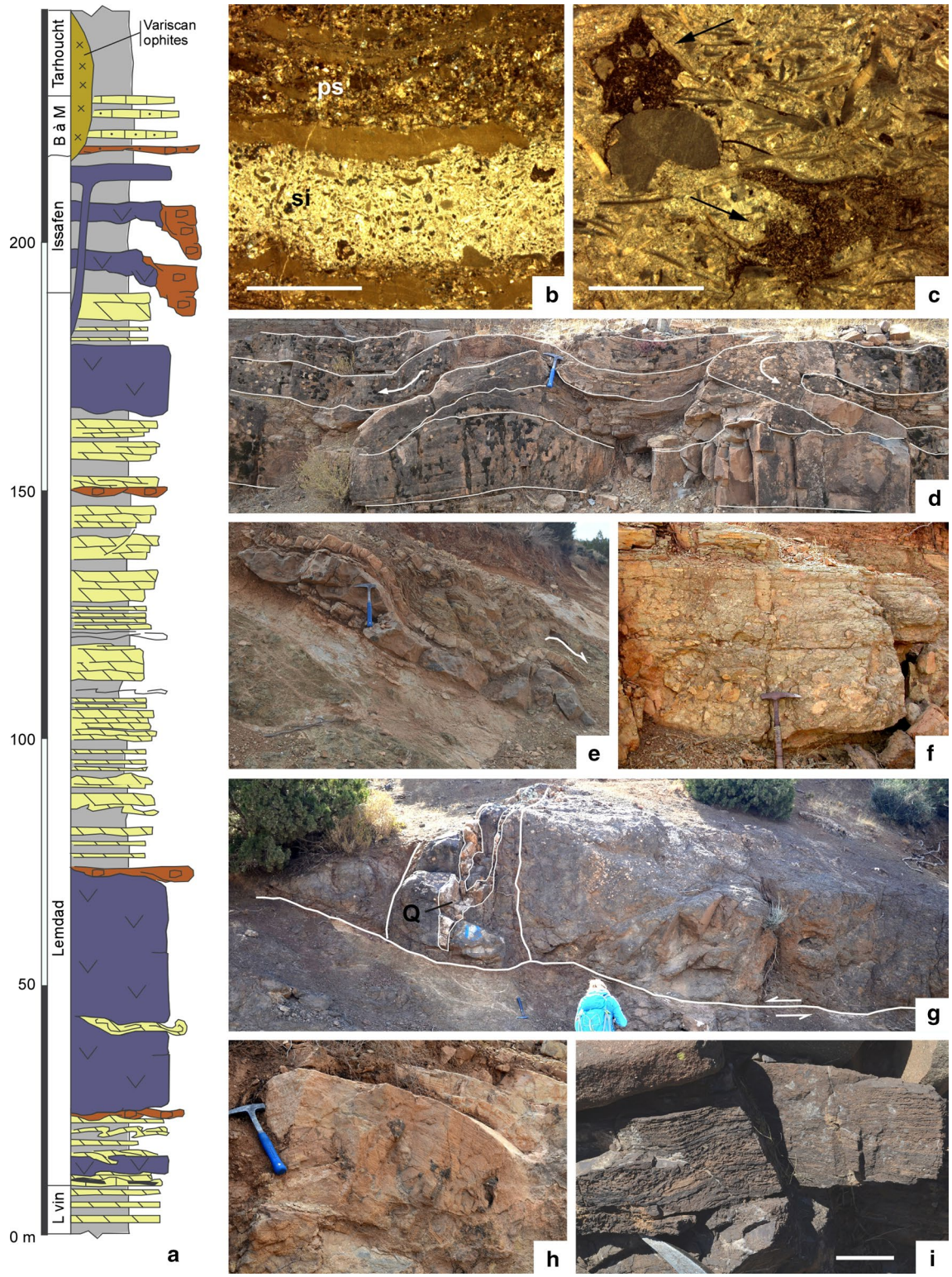

(core) parts are less vesicular and poorly jointed, whereas the basal and upper crusts are oxidized, highly vesicular and either close to brecciation or brecciated. Flows commonly pass laterally into clast-supported, breccia sheet-like units and lobes with channelled cross sections, up to 2.2 m thick (Fig. 4f). They consist of poorly sorted, angular to subrounded, (polymictic) porphyritic, pebble-to-granule clasts embedded in a coarse-grained to silty tuff matrix. NE–SW-striking feeder dykes are subvertical and can be followed laterally for c. 1 km (Figs. 3a, 4g). The dykes

◀ **Fig. 4** Tamdroust Volcanic Complex. **a** Stratigraphic log of the Lemdad-to-Tarhoucht lithostratigraphic units showing thickness and emplacement of lava flows and Permian ophites; Lvin-Lie-de-vin Formation, BàM-Brèche à Micmacca Member; same legend than previous figure. **b** Photomicrograph of a carbonate slumped bed showing an alternation of calcarenites, rich in muddy intraclasts and volcaniclasts, and volcaniclastic mudstone reflecting diagenetic alternation of silicified (si) and partly silicified (ps) couplets; scale = 5 mm. **c** Photomicrograph of a grainstone rich in echinoderm ossicles, calcite-walled brachiopod valves, trilobite sclerites and hyoliths, and displaying secondary dissolution vugs (*arrowed*) occluded with a mixture of intraclasts and bioclasts of smaller size cemented by haematite; scale = 3 mm. **d** Superposition of sliding and slumping carbonate strata of the Lemdad Formation embedding contorted (*folded*) beds; *arrows mark* slope direction. **e** Conglomeratic channel capped by gravel-rich litharenitic laminated beds. **f** Slumping and sliding, carbonate and shale beds of the basal Lemdad Formation. **g** Feeder dyke of (*lateral*) lava flows affected by inverse fault (probably Variscan in age) affecting both the dyke, the lava flows and the encased hydrothermal (quartzite, Q) dykes and veins. **h** Stromatolite bioherms of the Lemdad Formation. **i** Silty limestone of the Brèche à Micmacca Member showing low-angle and trough-cross lamination

crosscut both carbonate/shale alternations of the Lemdad and Issafen Formations and previous lava flows. Their contacts with the country rock are very distinct although, in some cases, one of the walls is not visible by faulting onset or soil cover. Master dykes commonly splay into anastomosing branches almost wholly filled with mafic lava and secondary and subsidiary, hydrothermal quartzitic dykes (Fig. 4g). Dyke offsets across layers of contrasting mechanical properties (e.g. dolostone/shale and basalt/shale contacts) are common.

Interbedded, clast-supported, polymictic conglomerates are interpreted as autoclastic breccia and derived conglomerates. The axial planes of the slump folds strike NE–SW (average trend about N30–60°) and dip moderately NW. These directions broadly coincide with preferential dyke strikes of N–S (340–35°) and N–S-striking palaeocurrents of channel axes (0–40°). Composite NNE–SSW basin-floor tilt and extension are suggested as a result of sharp subsidence events. This direction matches with striking directions of extensional components reported across the Ediacaran–Cambrian transition in neighbouring areas of the southern High Atlas (Pouclet et al. 2007; Soulaimani et al. 2014). Differential subsidence events owing to NNE–SSW extension can be related to readjustment of underlying rift blocks. Finally, the Tamdroust Volcanic Complex palaeorelief is onlapped by the Brèche à Micmacca Member (Figs. 2, 3a, 4i).

Bab n'Ali Volcanic Complex

The presence of a distinct volcanosedimentary unit bordering the southern Saghro inlier, different from the classical Ouarzazate Supergroup and "lower Cambrian" strata, was already reported by Hindermeyer et al. (1977), who mapped it as Triassic dolerites. Hawkins et al. (2001) and O'Connor (2010) constrained the extension of Triassic dolerite dykes and sills and, due to its stratigraphic position, defined the so-called Bab n'Ali Formation as a coarse-grained terrigenous unit overlying the Ediacaran Ouarzazate Supergroup and other underlying "lower Cambrian" Formations. The authors tentatively suggested the lateral equivalence of the Bab n'Ali Formation to the Tikirt Member of the Lie-de-vin Formation (for a lithostratigraphic revision of the entire Anti-Atlas, see Álvaro et al. 2014a). Although the stratigraphic subdivision of the mapped units related to the complex is exclusively lithostratigraphic, and their respective age is in need of radiometric dating confirmation, we will follow below Hawkins et al. (2001) and O'Connor's (2010) stratigraphic framework. According to Hawkins et al. (2001), the Bab n'Ali Complex or Formation is up to 50 m thick and unconformably overlies different Neoproterozoic units, such the Imlas Group (Ouarzazate Supergroup) and

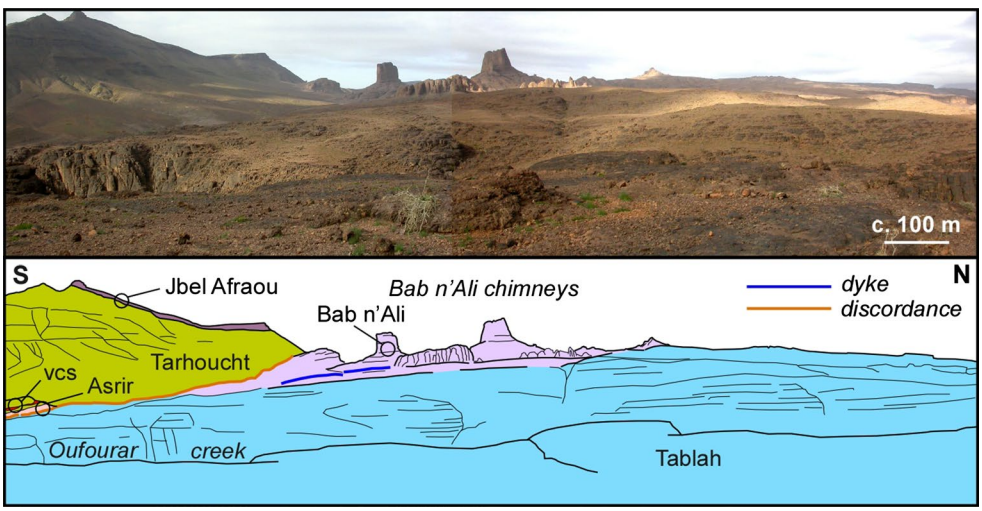

Fig. 5 Panoramic view of the southern Bab n'Ali Complex, cross section of the geographical and lithostratigraphic terms reported in the text, and onlapping relationship with the Asrir and Jbel Wawrmast formations; vcs: embedded volcanosedimentary channels

the Ikniwn Granodiorite. According to our observations, which differ from the aforementioned reports, the complex is directly overlain by the Tislit, Asrir and Jbel Wawrmast Formations in a progressive onlapping framework (Figs. 2, 3b, 5).

The Bab n'Ali volcanosedimentary complex is dominated by bedded and chaotic breccias and tuffs that extend, at least, across c. 10 km, along a W–E-trending oued that connects the villages of Berkik (other used toponymies are Barkik and Berkouk) and Ikfrane (or Ain Ikefran) and the Bab n'Ali (geomorphological) chimneys (Fig. 3b). Although the original extent of the volcanosedimentary unit cannot be properly ascertained, because it is dissected by faults and scoured by transverse oueds and rivulets, remnants of the volcanosedimentary apron form a plano-convex edifice with elliptical cross section of 10 × 6 km. Eruptive centres of the volcanic edifice are not well constrained, although some potential N–S-striking feeder dykes occur crosscutting the sedimentary aprons but not the onlapping Jbel Wawrmast Formation (Figs. 5, 6d).

Oueds eroding the E–W-trending complex edifice allow identification of sharp changes of underlying and overlying strata. In the vicinity of the Bab n'Ali chimneys and the Oufourar creek, the complex overlies two acidic volcanosedimentary units, bounded by erosive unconformable contacts, whose assignation to the Imlas Group (Ouarzazate Supergroup) is also in need of radiometric confirmation. Hawkins et al. (2001) named them the Tablah (a conglomerate-dominated unit; Figs. 2, 5) and Akhmassi/Assaka Formations (rhyolitic ignimbrites; Fig. 6a–d), respectively. The Assaka Formation unconformably overlies a complex of basic lava flows associated with hydrothermal dykes (Tifkhsit Formation of Imlas Group; Fig. 6a). In the study area, neither the Adoudou nor the classical Lie-de-vin Formation is identified, so the identification of a single (associating the Akhmassi/Assaka, Tablah and Bab n'Ali units) or composite acidic episode across the Ediacaran–Cambrian transition cannot be ascertained based exclusively on lithostratigraphic relationships (Fig. 2). Independently of the assignation of the Tablah, Assaka and Akhmassi Formations to the Ediacaran Ouarzazate Supergroup or the "lowermost Cambrian" Taroudant Group, our interest is focused on the own Bab n'Ali volcanosedimentary complex and its cover, which are described below.

The Bab n'Ali Volcanic Complex consists of massive- to thick-bedded, moderately sorted and clast-supported to poorly sorted and matrix-supported, tuff, lapilli tuff, conglomerate and breccia (Fig. 6e) with interbedded lava flows and dykes (Fig. 5f). Beds range from structureless to normal and reverse graded. Clasts are angular to subrounded and include scoria to non-vesicular fine to coarse lapilli, and non-vesicular to slightly vesicular fine to medium blocks and bombs and a wide diversity of polymictic clasts

Fig. 6 **a** Top of the Tifkhsit Formation with a hydrothermal dyke (*arrowed*) sealed by ignimbrites of the Akhmassi Formation; Oufourar creek. **b** Typical aspect of the pinkish ignimbrites of the Akhmassi Formation reflecting diagenetic alternations of whole and partial silicification processes; Oufourar creek. **c** Rhyolitic bomb embedded in the Akhmassi ignimbrites; Oufourar creek. **d** Erosive discontinuity (*arrowed*) of the Tifkhsit/Akhmassi contact; Oufourar creek. **e** Chimneys of Bab n'Ali showing crudely stratified, unselected, conglomerates and breccias of the homonymous formation. **f** Lava flow embedded in matrix-supported breccias of the Bab n'Ali Formation. **g** Unsorted, grain-supported conglomerate bed of the Bab n'Ali Volcanic Complex apron. **h** Probable feeder dyke (*width marked*) crosscutting the volcanosedimentary apron of the Bab n'Ali Volcanic Complex at the homonymous site (N31°02′58.49″ W05°48′58.39″); Oufourar creek: ignimbrites, N31°41′03.63″ W05°47′59.80″ and N31°03′51.77″ W05°47′41.77″; lava flows: N31°04′08-24″ W05°48′11.29″

sourced from the basement (Fig. 6g). Matrix is fine ash (silt) to coarse ash (coarse to very coarse sand). Distinct belts of pyroclastic breccia to tuff breccia (proximal) and lapilli to lapillistone (distal) occur radially from the complex axis.

The southern margin of the Bab n'Ali edifice is onlapped by the Tislit and Asrir Formations and even the Brèche à Micmacca and Tarhoucht Members of the Jbel Wawrmast Formation (Figs. 3b, 5). The Tislit Formation, which directly onlaps both the Tablah and Bab n'Ali Formations, is up to 30 m thick in the study area and consists of thick-bedded alternations of siltstone/fine-grained sandstone couplets with currently interbedded conglomeratic channels and rhyolitic tuffs (Fig. 7a). The litharenites are dominated by rounded to subrounded lithoclasts, many of them volcanosedimentary in origin (Fig. 6b, c). Sedimentary structures are dominated by low-angle and parallel lamination, symmetric and asymmetric ripples, trough cross-laminated sets up to 10 cm thick. Burrowing traces are not observed. Strata can be scoured by lobes (Fig. 7b), with elliptical cross section, up to 10 m in diameter and 6 m thick. Original slopes were affected by gravitational instability and resedimented depending primarily on gravity-driven processes. The heterogeneous composition of volcanic lithic grains and the abundance of shallow-water bottom energy indicate that the sediment was derived from erosion of subaerial volcanic deposits subsequently remobilized in alluvial and fluvial environments.

The overlying Asrir Formation crops out, at least, along the southern margin of the Bab n'Ali Volcanic Complex (Figs. 3b, 5, 7c, d). It is up to 12 m thick and consists of amalgamated, litharenitic, channels and shoals displaying multidirectional trough and cross-stratification, parallel and low-angle laminae, symmetric ripples and local grading reflecting migration of bedforms in a high-energy setting, probably fluvial in character.

It is noticeable the distinctive facies of the Brèche à Micmacca Member onlapping the Bab n'Ali Volcanic

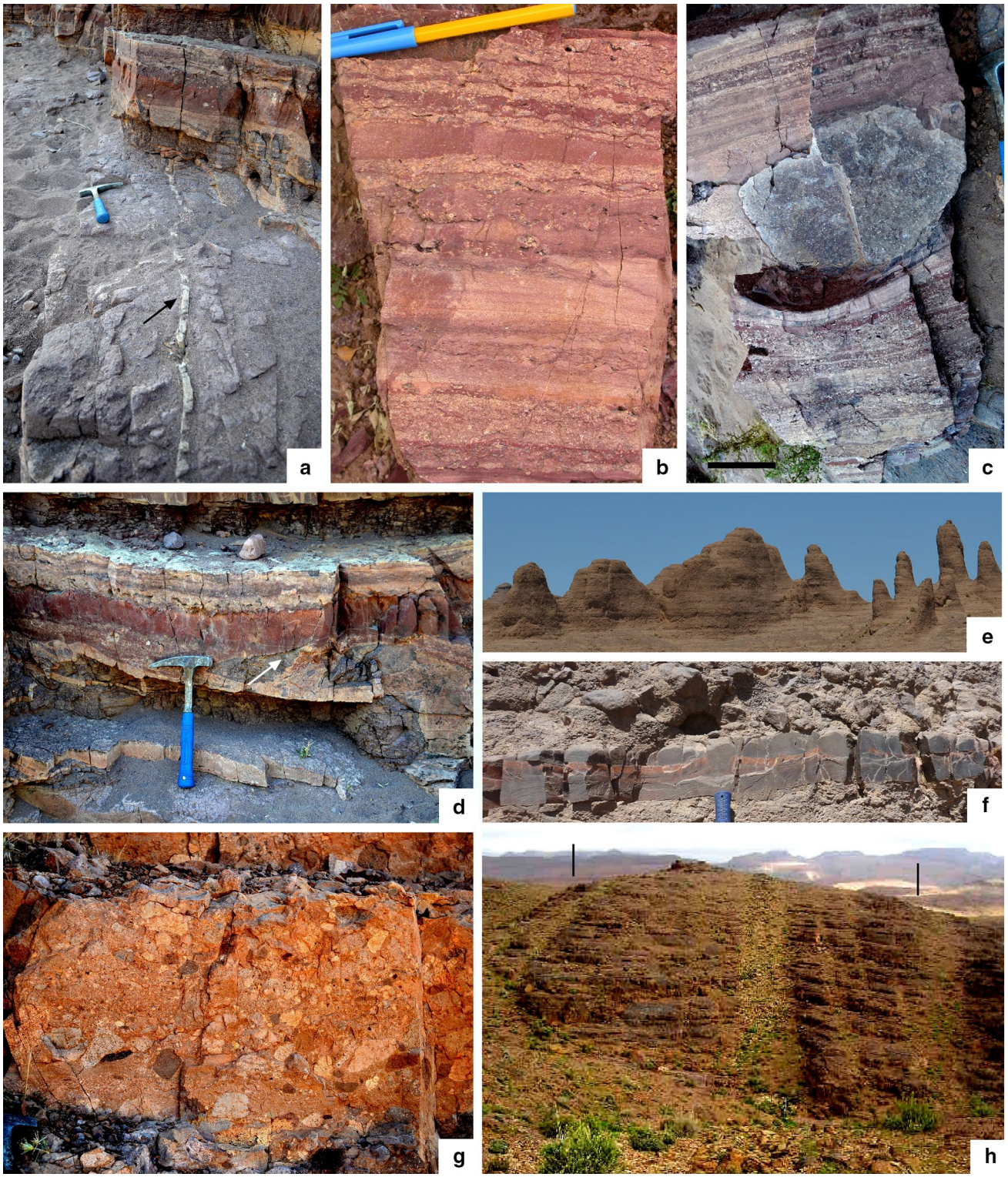

Complex, which exhibits some distinct sedimentary structures uncommon in other exposures. Brownish, thin-bedded, impure dolostones are discontinuously exposed as a belt surrounding, at least, the southern Bab n'Ali Volcanic Complex (Fig. 3b). They show parallel and low-angle laminae, trough cross-stratified sets, up to 20 cm thick, and common symmetric ripples lining the top of beds (Fig. 7e–g). The impure character of these dolostones is controlled by variable proportions, up to 40 % in volume, of allochems, such as quartz, feldspar, opaque and mafic clasts derived from the substrate. The dolostones of the Brèche à Micmacca Member represent

Fig. 7 **a** Aspect of the Tislit litharenites (lower beige cross-stratified sandstones and upper grey unsorted conflomerates) overlain by the Asrir Formation and the Brèche à Micmacca Member at the NW edge of the Bab n'Ali volcanosedimentary Complex. **b** Lobe-shaped olistostrome of the Tislit Formation (*arrowed*). **c** Erosive Tislit/Asrir contact. **d** Multidirectional cross-stratified sandstones with foreset and channel surfaces marked with shaly clasts; Asrir Formation. **e** Stratigraphic superposition of the Asrir-to-Jbel Afraou formations close to Berkik. **f** Asrir-to-Tarhoucht transition showing the replacement of the Brèche à Micmacca dolostones by volcanosedimentary channels representing reactivated erosive pulses on the Bab n'Ali palaeorelief. **g**, **h** Anomalous Brèche à Micmacca Member showing superposed trough cross- and low-laminated sets of (volcaniclastic) silty dolostones; *As* Asrir, *BaM* Brèche à Micmacca, *JA* Jbel Afraou, *Ta* Tarhoucht Member, *vcs* volcanosedimentary interbed

here foreshore-to-shoreface environments lacking skeletal influence. In some exposures lacking these dolostones, the latter are replaced by volcanosedimentary conglomeratic lenses and channels, up to 2 m thick, which occur embedded in the lowermost shales of the overlying Tarhoucht Member (Figs. 5, 7e, f). Finally, the latter member represents a blanket sealing previous palaeotopographies.

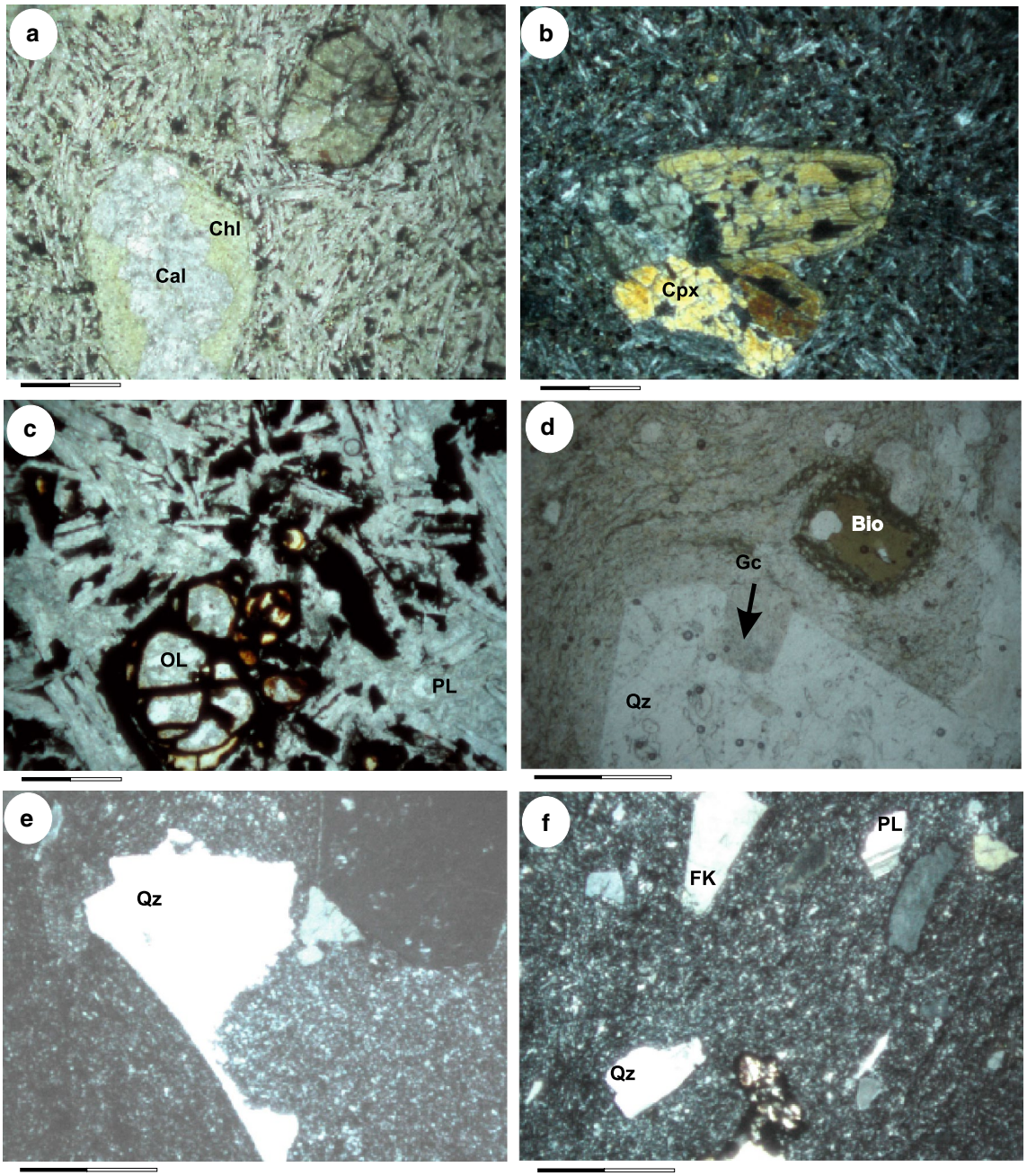

Fig. 8 Thin-section photomicrographs of the volcanic rocks described in the text. **a** Vacuolar microlithic texture of a basalt from Bab n'Ali; note the sequential filling of vacuoles (chlorite to calcite); nl. **b** Clinopyroxene clustered syneusis texture in a basalt from Tamdroust; pl. **c** Intersertal texture with completely altered olivine; nl. **d** Corroded quartz in a rhyolite from Bab n'Ali; nl. **e** Dissolved quartz in the ignimbritic rhyolite of Bab n'Ali; pl. **f** Tuffic rhyolite from the Lemdad area; pl. Acronyms *nl* normal light and *pl* polarized light, *Bio* biotite, *Cal* calcite, *Chl* chlorite, *Cpx* clinopyroxene, *FK* K-feldspar, *Gc* corroded gulf, *OL* olivine, *PL* plagioclase, *Qz* quartz; scales = 0.5 mm (**a**, **c**), 0.6 mm (**b**) and 1 mm (**d**–**f**)

Volcanic products: petrography and geochemistry

An homogeneous basic volcanic pulse is identified in the Tamdroust Volcanic Complex, whereas two volcanic products are distinguished in the Bab n'Ali Volcanic Complex: (1) the reported basic N–S-striking feeder dykes (in need of radiometric confirmation) that crosscut the Bab n'Ali sedimentary apron, but not the onlapping Jbel Wawrmast Formation and (2) the acidic volcanic bombs, lava flows and interbedded rhyolitic tuffs of the apron:

1. The basic volcanic episodes of the Tamdroust and Bab n'Ali Volcanic Complexes are mainly effusive and related to lava flows and feeder dykes. These show microlithic vacuolar (Fig. 8a) and porphyritic (Fig. 8b) textures, changing locally into intersertale in the vicinity of dykes (Fig. 8c). Phenocrysts are dominated by plagioclases and clinopyroxenes. The former are mainly sericitized and, in Bab n'Ali, albitized. The latter are also broadly replaced by chlorite, epidote and iron oxides in Bab n'Ali, whereas they are better preserved in Tamdroust, where phenocryst clusters commonly display syneusis textures (Fig. 8b). The microlitic groundmass contains plagioclase, iron oxides and relics of olivine microphenocrysts, recognizable by their alteration products composed of a mixture of clay mineral and iron oxide mosaics (Fig. 8c).
2. The acidic volcanic episode of the Bab n'Ali Volcanic Complex, of explosive character and volumetrically dominant, is characterized by pyroclastic rocks with (undated) interbedded lava flows and pinkish rhyolitic tuffs. Phenocrysts are dominated by corroded quartz (Fig. 8d) locally exhibiting re-absorption/re-equilibrium features (Fig. 8e), K-feldspar, plagioclase and biotite, the latter partly altered to chlorite. Locally, the rhyolitic tuffs show fragmented (pyroclastic) textures that involved cataclasis of crystals (Fig. 8f), a feature characteristic of ignimbrites.

Geochemically, the basalts (mainly dykes) from Bab n'Ali show higher contents in SiO_2 (51–55 %), Al_2O_3 (20–22 %) and $K_2O + Na_2O$ (14–17 %) and lower in MgO (0.2–0.5 %), Fe_2O_3 (3 %), CaO (1–3 %) and TiO_2 (0.4 %) than those of Tamdroust (SiO_2 = 44–52 %; Al_2O_3 = 13–19 %; $Na_2O + K_2O$ = 4–8 %; MgO = 3–12 %; Fe_2O_3 = 9–12 %; CaO = 1–10 % and TiO_2 = 2 %) (Table 1). Although the alkali content of the basalts from Bab n'Ali suggests an alkaline character, their $K_2O + Na_2O/Al_2O_3$ ratio is <1; their high content in Na_2O (8–11 %), Na_2O/K_2O >1 relationship and depleted contents in CaO (1–3 %) can be explained as a result of conspicuous albitization processes controlled by hydrothermal and metamorphic processes. By contrast, the acidic rocks (mainly rhyolitic tuffs) show higher contents in SiO_2 (74–81 %) coeval with lower values of MgO (0.1–1 %), Fe_2O_3 (2 %) and CaO (1–4 %).

In the Nb/Y versus Zr/TiO_2 diagram of Winchester and Floyd (1976, 1977), most of the basic products plot within the field of basalts (Tamdroust) and andesitic basalts (Bab n'Ali), whereas all the acidic rocks are rhyolites (Fig. 9a). A comparison of the index of differentiation (#Mg) suggests a more differentiated liquid source for the andesitic basalts of Bab n'Ali (#Mg < 20) than for the basalts of Tamdroust (#Mg = 35–60). The lower values of #Mg coincide with lower contents in Ni and Cr suggesting higher levels of olivine and pyroxene fractionation. The AFM diagram and the Nb/Y index (Fig. 9b), which are considered as unaffected by alteration and metamorphic processes, suggest a tholeiitic affinity for the Tamdroust and Bab n'Ali volcanic episodes. They are plotted in a typical within plate setting, in agreement with the Zr versus Zr/Y diagram after Pearce and Norry (1979) (Fig. 9c).

The spider-diagrams of the andesitic basalts from Bab n'Ali show pronounced negative anomalies in Sr and Ti ($Ti/Ti^* = 0.15–0.26$) (Fig. 9d) that suggest great fractionation patterns of plagioclase, ferromagnesian minerals and iron–titanium oxides. They also display an enrichment in light REE (LREE) (La/Sm > 10) with a flat profile of heavy REE (HREE) from Gd to Yb, and a ratio Zr/Hf < 10. By contrast, the basalts of Tamdroust show the ratios La/Sm < 10 and Zr/Hf > 37 and fractionated HREE contents (Fig. 9e).

The spider-diagrams of the acidic rocks are parallel to those of their preceding basalts, with stronger anomalies in Sr, Ti and Zr related to important fractionation of plagioclases, iron–titanium oxides and zircons (Fig. 9d, e). The parallelism in the basic and acidic profiles suggests that early basaltic and later felsic volcanism were congenetic in the Bab n'Ali Volcanic Complex.

In addition, the ratio $(Gd/Yb)_{nC}$ is useful to characterize the nature of the magmatic source, as a ratio >2 suggests partial fusion of a garnet-bearing source (Ellam 1992; Fitton et al. 1997; Fergusson et al. 2009; Rooney 2010). According to this ratio, the reported basalts can be subdivided into: (1) an andesitic basaltic group from Bab n'Ali Volcanic Complex, with $(Gd/Yb)_{nC}$ <2 and suggesting lack of garnet-bearing sources and (2) a basaltic group of Tamdroust Volcanic Complex, with $(Gd/Yb)_{nC}$ >2 and implying melting of a garnet-bearing source. Therefore, the Tamdroust Volcanic Complex basalts derived from a deeper source than those of Bab n'Ali Volcanic Complex. The latter would represent a volcanism that took place in a more evolved rift, as suggested by their plotting in the plate-margin domain of Pearce and Gale's (1977) diagram, close to Holm's (1985) initial rifting tholeiite (IRT) point (Fig. 9h).

Despite their somewhat similar negative anomalies in Nb and Sr, the spider-diagrams of the basaltic rocks from Bab n'Ali are completely different to those of the underlying Tifkhsit Formation (Imlas Group), late Ediacaran in age (Table 1; Fig. 9f). The Cambrian basalts are more fractionated (La/Yb > 14) than the Ediacaran ones (La/Yb < 14), which display higher values of LREE and a flat profile of HREE (from Gd to Yb). By contrast, the spider-diagrams of Bab n'Ali and Tamdroust are similar to those of the continental tholeiite from Sabie River, South Africa (Marsh 1987), sharing common anomalies in Nb and Ti and lower fractionation patterns in HREE (Fig. 9f, g). The anomalies in Nb and Ti, characteristic of continental tholeiites, are absent in the lowermost Cambrian alkaline basalts of the

Table 1 Chemical analyses of 23 samples from the uppermost Ediacaran to Cambrian volcanic rocks of the Bab n'Ali and Tamdroust volcanic complexes

	Bab n'Ali Volcanic Complex													
	Basement of the Ouarzazate Supergroup				Lower Cambrian edifice									
	TO2	TO4	BA9	Bk3/5	TO6	BA7	BA7b	OUS3	Bk4	OUS1	OUS5	OUS6	OUS1b	Bk4/2
SiO_2	46.89	51.55	44.62	46.41	51.62	55.33	55.93	53.23	51.55	78.33	73.78	76.03	80.78	72.57
TiO_2	2.35	1.89	2.16	2.01	0.4	0.37	0.35	0.41	0.42	0.39	0.35	0.29	0.33	0.24
Al_2O_3	15.2	15.66	16.23	14.47	22.13	20.13	20.21	20.45	20.3	9.53	9.49	9.21	8.86	11.86
$Fe_2O_3^a$	11.19	9.4	11.05	10.23	3.18	3.5	3.32	3.46	3.61	1.69	2.17	2.01	1.81	2.27
MnO	0.4	0.2	0.37	0.27	0.17	0.22	0.22	0.26	0.27	0.03	0.07	0.06	0.04	0.06
MgO	7.22	5.71	7.74	5.05	0.26	0.3	0.21	0.58	0.51	0.4	1.15	1.44	0.31	0.09
CaO	5.23	3.15	4.09	6.09	1.26	1.03	0.9	2.44	3.57	0.83	3.86	2.29	0.68	2.18
Na_2O	4.84	5.71	3.73	4.00	10.74	8.21	8.44	11.15	10.91	0.84	1.39	1.53	0.71	5.41
K_2O	2.14	2.15	3.17	4.03	6.3	6.35	5.91	3.25	3.2	4.39	2.93	2.67	4.1	2.15
P_2O_5	0.42	0.35	0.37	0.36	0.07	0.01	0.03	0.05	0.17	0.1	0.08	0.07	0.08	0.01
LOI	3.28	2.78	5.76	6.8	2.86	4.34	4.28	4.12	4.5	1.97	4.6	3.34	2.14	2.4
Total (ppm)	99.16	98.54	99.29	99.73	99.00	99.78	99.8	99.4	99.01	98.49	99.88	98.94		99.2
Ba	415	1,569	1,677	650	374	103	42	571	474	523	483	470	511	5,497
Rb	56	66	134	100	176	225	244	128	120.8	74	98	89	77	35.2
Sr	206	387	253	164	784	271	262	907	1,235	56	61	63	42	324
Y	35.3	34.6	29.2	40.9	15.6	25	20	25	27.6	18.2	17.2	13.4	20	25.1
Zr	206	236	198	186.2	86.8	133	142.3	135.3	121.8	189	207	152	191	348.2
Nb	11.2	9	13	9.8	3.7	7.2	7.7	7.4	6.6	6.1	6.4	5.7	6	15.9
Zn	a	a	a		a	a				a	a	a		
Ni	110	40	130	70	20	20				20	20	20		
Cr	100	200	140	<20	20	20				30	30	30		<20
Ta	0.7	0.5	0.7	0.5	10.6	22.8	2.7	2.5	17.4	0.4	0.4	0.4		1.2
Co	33	25	37	26	2	1			0.6	3	6	10		
Hf	4.5	4.9	4.2	4.1	10.7	16.6	14	15	14.7	4.2	3.7	3.7		8.7
Th	1.03	2.47	1.15	0.9	41.4	92.7	83	55	67.1	5.63	6.2	5.3	8	15
U														
V				180					77					68
La	25.6	14.6	16.6	44.1	43.4	45.5			125.5	17.5	18.6	14.3		30.4
Ce	57.9	37.5	42.1	78.6	76	86.1			203	36.2	32.2	32.2		76.3
Pr	7.06	4.91	5.39	11.31	6.61	7.65			17.59	4.33	3.94	3.94		8.52
Nd	30.7	22.6	23.9	48.6	20.2	22.8	27	51	52.2	17	15.4	15.4	22	32.6
Sm	6.7	5.51	5.7	9.87	3.05	3.66	6	10	6.68	3.51	3.05	3.05	7	6.44
Eu	1.98	1.63	1.83	1.78	0.87	1.15			1.98	0.64	0.59	0.59		0.76
Gd	6.21	5.45	5.49	10.08	2.22	3			5.54	3.13	2.56	2.56		5.93
Tb	1.06	0.95	0.89	1.34	0.37	0.57			0.82	0.5	0.41	0.41		0.84
Dy	6	5.71	5.18	7.71	2.28	3.63			4.79	2.75	2.29	2.29		5.13
Ho	1.21	1.14	1.03	1.36	0.48	0.79			1.01	0.55	0.43	0.43		1.03
Er	3.31	3.22	2.87	3.26	1.49	2.65			3.13	1.59	1.23	1.23		3.27
Tm	0.49	0.49	0.42	0.48	0.25	0.48			0.5	0.24	0.19	0.19		0.55
Yb	3.02	3.13	2.69	2.97	1.89	3.53			3.57	1.62	1.25	1.25		3.42
Lu	0.47	0.5	0.43	0.45	0.33	0.59			0.6	0.26	0.21	0.21		0.52

Table 1 continued

	Tamdroust Volcanic Complex								
	Lava flows and dykes								
	Tam1	Tam3	Tam5a	Tam5b	Tam6	Tam7	Tam10	Tam28	Tam30
SiO_2	46.06	46.71	44.1	47.36	46.54	48.34	47.21	52.4	52.98
TiO_2	2.15	1.81	1.45	1.51	2.395	2.431	2.436	2.2	2.162
Al_2O_3	19.55	16.49	13.28	14.82	15.77	16.06	16.1	16.89	15.51
$Fe_2O_3^a$	10.48	10.25	10.51	12.59	11.41	10.43	11.35	9.59	9.15
MnO	0.03	0.18	0.09	0.08	0.17	0.13	0.2	0.21	0.15
MgO	12.62	7.09	8.18	10.4	6.31	6.2	6.05	3.75	3.13
CaO	0.91	7.07	10.58	5.04	8.07	9.34	7.31	5.17	3.86
Na_2O	2.87	1.81	3.89	4.1	2.8	3.24	2.91	6.02	5.4
K_2O	1.79	4.44	0.19	0.24	2.61	1.83	2.97	1.09	1.27
P_2O_5	0.34	0.25	0.2	0.2	0.46	0.48	0.49	0.36	0.4
LOI	3.91	3.39	5.95	4.27	3.04	2.2	3.02	2.67	4.88
Total (ppm)	100.7	99.51	98.42	100.6	99.56	100.7	100.00	100.3	98.89
Ba	147	975	107	121	908	435	1,581	322	3,453
Rb	15	60	2	2	39	27	43	11	15
Sr	91	1,117	133	110	1,229	644	1,087	348	255
Y	24.4	21.4	17.8	16.9	27.3	28.4	28.6	28.8	33.7
Zr	142	138	85	90	147	152	152	174	208
Nb	10.5	9.5	5.6	5.8	8.3	8.4	8.7	8.3	9.9
Zn	130	100	110	130	100	80	120	190	90
Ni	60	100	170	200	60	60	60	20	20
Cr	60	170	350	360	70	70	70	<20	<20
Ta	0.7	0.9	0.4	0.3	0.8	0.7	0.9	0.6	0.7
Co	41	51	31	40	48	40	54	20	16
Hf	3.1	3.2	2.1	2.1	3.5	3.5	3.5	4.2	4.8
Th	1.23	1.12	0.61	0.63	1.56	1.55	1.53	1.98	2.33
U	0.72	0.68	0.45	0.4	1.08	1.06	1.07	1.49	1.73
V	293	271	201	232	378	358	368	237	203
La	14.5	12.3	10.2	8.61	19.2	19.8	19.7	16	18.3
Ce	35.9	31.7	25.9	21.5	50.9	51.4	51.4	40.8	47
Pr	4.46	4.11	3.4	2.82	6.84	6.97	6.94	5.34	6.22
Nd	19.8	19	15.9	13.3	32.3	33.4	32.6	25	28.6
Sm	4.66	4.67	3.82	3.57	7.58	7.81	7.63	6.04	7.09
Eu	1.4	1.49	1.22	1.12	2.39	2.42	2.43	1.99	2.13
Gd	4.63	4.54	3.8	3.32	6.55	6.66	6.58	5.64	6.43
Tb	0.77	0.73	0.59	0.54	0.99	0.98	0.97	0.94	1.05
Dy	4.41	4.03	3.28	3.05	5.19	5.16	5.29	5.32	6
Ho	0.86	0.78	0.62	0.58	0.96	0.97	0.95	1.01	1.15
Er	2.27	2.08	1.63	1.55	2.58	2.59	2.61	2.91	3.18
Tm	0.311	0.302	0.23	0.218	0.345	0.361	0.359	0.428	0.478
Yb	1.91	1.96	1.42	1.37	2.18	2.23	2.2	2.81	3.12
Lu	0.3	0.3	0.22	0.21	0.35	0.34	0.35	0.44	0.5

Analyses were carried out using X-ray fluorescence (XRF) at the certified laboratories of INETI, Porto (Portugal) and AcmeLabs, Canada. Analytical uncertainties are calculated to 2 % for major elements and 5–10 % for trace elements. Lambert coordinates of these samples are as follows: TO2 and Bk3/5 (N31°4.8′, W5°48.6′), BA9 and TO4 (N31°4.5′, W5°48.3′), TO6, BA7 and BA7b (N31°3.5′, W5°47.7′), OUS3 (N31°3.5′, W5°48.4′), Bk4 and Bk4/2 (N31°1.7′, W5°54′), OUS1 and OUS1b (N31°3′, W5°49′), OUS5 and OUS6 (N31°3.3′, W5°48.7′), Tam1 and Tam3 (N30°56′, W8°7.8′), Tam5a, Tam5b and Tam6 (N30°56.3′, W8°7.5′), Tam7 and Tam10 (N30°55.8′, W8°7.5′), and Tam28 and Tam30 (N30°55.3′, W8°7.8′)

LOI loss on ignition

[a] Total iron as Fe_2O_3

Jbel Boho (Álvaro et al. 2006) and the middle Cambrian alkaline basalts of the Moroccan Meseta (Álvaro et al. 2008a). This anomaly in Nb displayed by intracontinental tholeiites is commonly interpreted as a result of crustal contamination (Bertrand et al. 1982; Marsh 1987; Zhou et al. 2004; Pearce 2008). A ratio La/Nb >1 is also characteristic of continental tholeiites and suggests different degrees of contamination (Wilson 1994). The continental setting of the tholeiites described in Tamdroust (Ouzellagh promontory, High Atlas) and Bab n'Ali (central Anti-Atlas) fits well with the geodynamic model established for the late Ediacaran–Cambrian Atlas Rift, recently summarized, among others, by Gasquet et al. (2005), Ezzouhairi et al. (2008) and Álvaro et al. (2014b).

Unconformities and geodynamic context

Because of the lack of radiometric constraints in the Bab n'Ali area, it is not possible to identify the end of the WCadomian Orogeny (third episode of the Pan-African Orogeny sensu Hefferan et al. 2014) currently associated with the onset of the Ouarzazate Supergroup. There, the top of the Tikhirst Formation marks the end of a basic volcanic episode (mainly represented by calk-alkaline lava flows, sills and dykes) associated with the emplacement of a hydrothermal network. After sealing of this palaeorelief (Fig. 6a), the overlying Assaka/Akhmassi units represent the record of acidic ignimbritic episodes (including volcanic bombs; Fig. 6c) and the erosion of previous palaeoreliefs, subsequently overlain by conglomerate and breccia sheets and lobes (Tablah Formation). The Bab n'Ali volcanosedimentary complex seems to represent a stepwise or a renewed episode of acidic explosive volcanic activity and palaeorelief erosion. In any case, both the Adoudou and Lie-de-vin Formations (representative of microbially mediated, peritidal-dominated, stable rift branches) and the centres of carbonate productivity developed during the rest of the "early Cambrian" in the western Anti-Atlas and southern High Atlas (Igoudine, Amouslek, Lemdad and Issafen Formations) are absent here. By contrast, the Bab n'Ali Formation is progressively onlapped by the fluvial–alluvial strata of the Tislit Member, the Asrir Formation and, where present, a special foreshore-to-shoreface facies association of the Brèche à Micmacca Member. Distinct offshore-dominated, marine conditions were only recorded by the blanket of previous palaeoreliefs (Tarhoucht Member). As a result, the presence of low-angle discordances (in fact, onlapping geometries) marks many of the lithostratigraphic contacts throughout the Jbel Saghro.

At the scale of the entire Atlas Rift, a succession of syn-rift unconformities can be summarized across the "lower–middle Cambrian transition":

1. The onset of the fluvial–alluvial Tislit Formation in the central and eastern Anti-Atlas seems related to rejuvenation of source areas (Walsh et al. 2008, 2012; Álvaro et al. 2014a). In the southern Saghro inlier, the formation occurs onlapping complex volcanosedimentary palaeoreliefs.
2. Both the basal and upper contacts of the Asrir Formation, as well as other intraAsrir discontinuities (such as that separating the lower fluvial Tazlaft and the upper marine Tatelt members; Fig. 10a–c), are the result of the interplay between global eustatic sea-level fall (the so-called Hawke Bay, Daroca or Toyonian Regression; Álvaro and Vennin 1998) and onlapping patterns (Fig. 11).
3. The base of the Brèche à Micmacca Member and other volcano-bioclastic limestones embedded in the unit mark important syn-rift events throughout the entire Atlas Rift. The basal discontinuity is defined by angular truncation of the underlying units and represents a basement split into a mosaic of horst and grabens. The magnitude of erosion along the basal unconformity varies both locally within individual, intrablock, fault-bounded depocentres, and across and between fault blocks, ranging from the Ediacaran Ouarzazate Supergroup to the Cambrian Asrir Formation (Fig. 2). Palaeohighs were eroded more deeply than adjoining troughs, as a result of which the Brèche à Micmacca Member directly overlaps different stratigraphic units. Strata of the Asrir Formation were preserved only within downdropped grabens and half-grabens, where they were "protected" from erosion as complex fault-blocks evolved. Within such troughs, continuation or resumption of sedimentation produced essentially (para)conformable contacts with the overlying Brèche à Micmacca Member (Fig. 11). Elsewhere, correlative Brèche à Micmacca beds overlapped truncated strata and overstepped a peneplaned horst-and-graben palaeotopography, even resting on volcanosedimentary strata of the Ouarzazate Supergroup, which formed parts of eroded horsts or tilt blocks. Rapid growth and denudation of volcanic landforms caused radial erosion in drainage systems and supplied large volumes of sediment to neighbouring lowlands.
4. In the vicinity of the Bab n'Ali volcanosedimentary complex, the top of the palaeorelief was onlapped by consecutive strata of the Tislit, Asrir and Jbel Wawrmast Formations, resulting in an unconformable onlapping geometry that involved the older units capping the lower parts of the palaeorelief and the upper Tarhoucht Member covering the Bab n'Ali Volcanic Complex summit (Figs. 2, 5a, b, 6d). By contrast, in the Tamdroust Volcanic Complex, the volcanosedimentary palaeorelief is exclusively onlapped by the Brèche à Micmacca.

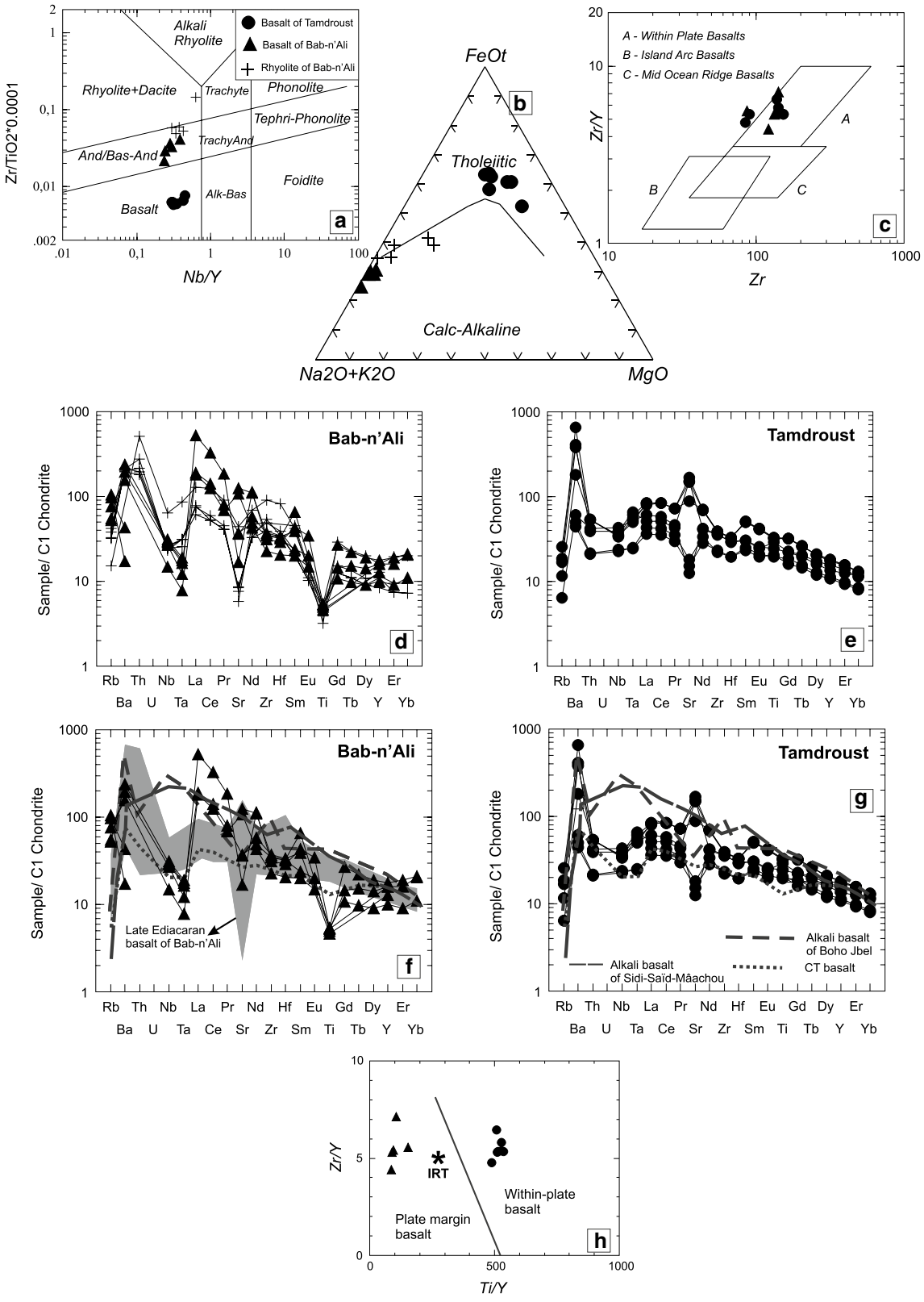

Although other "fossil rifts" support a simple threefold subdivision (pre-rift, syn-rift and post-rift/drift), others are marked by repeated syn-rift episodes of local tilting and uplift and separated by long intervals of quiescence. This seems to be the case of the Atlas Rift, in which, after a distinct latest Ediacaran syn-rift phase responsible for

◀ **Fig. 9** Discrimination diagrams and their spider-diagrams of analysed volcanic rocks. **a** Classification of studied rocks in Winchester and Floyd's diagram (1976, 1977). **b** AFM diagram, the boundary between the calc-alkaline field and the tholeiitic field after Irvine and Baragar (1971). **c** Zr–Zr/Y discrimination diagram for basalts (after Pearce and Norry 1979). **d**, **e** Multielement spider-diagrams of the Bab n'Ali and Tamdroust volcanic rocks normalized to C1 chondrite (Sun and McDounough 1989). **f**, **g** Chondrite C1 (Sun and McDounough 1989) normalized trace-element patterns for basalts from Bab n'Ali and Tamdroust compared to "lowermost Cambrian" alkali basalts of the Jbel Boho (Álvaro et al. 2006), "middle Cambrian" alkali basalts from Sidi-Saïd-Mâachou (Álvaro et al. 2008a) and continental tholeiite (CT) of the Sabie river (Marsh 1987). **h** Zr/Y versus Ti/Y discrimination diagram for basalts (Pearce and Gale 1977)

the onset of a distinct unconformity and angular discordance marking the top of the Taguedit Bed (Álvaro 2013), a quiescent episode led to sedimentation of the homogeneous, carbonate-dominated blanket of the Tifnout Member. This was succeeded by gentle changes in accommodation space controlling nucleation and development of reef and mud–mound complexes (Álvaro and Debrenne 2010), and local tilting and recording of biostratigraphically controlled gaps (Álvaro and Clausen 2007). A second episode recording distinct onlapping geometries and syn-rift pulses represented by the low-angle unconformities that mark the base of the Brèche à Micmacca Member, at least, in the central Anti-Atlas and the southern High Atlas. This can be associated with other erosive unconformities that (1) subdivide the Asrir Formation into continental-Tazlaft and marine-Tatelt Members (Buggisch and Siegert 1988; Álvaro and Clausen 2008; for another interpretation, see Landing et al. 2006) (Fig. 7a–c) and (2) the record of the volcano-bioclastic limestones that characterize the Brèche à Micmacca, which commonly display evidence of condensation events (Buggisch et al. 1978; Álvaro and Clausen 2006, 2008; Álvaro 2014). The vertical movements of the faults bounding some blocks, locally exceeded 200–400 m, led to non-deposition or erosion of the Adoudou and Lie-de-vin Formations, as a result of which the Brèche à Micmacca directly onlaps the Ediacaran Ouarzazate Supergroup. In other neighbouring areas, such as in the Jbel Arhouri, fringing the northern Jbel Saghro, the whole "lower Cambrian" is also missing, and the Ouarzazate/Brèche à Micmacca contact implies similar erosion patterns (Boudda et al. 1979; Geyer and Landing 1995; Álvaro and Clausen 2008). We suggest that this angular discordance-to-paraconformable contact is a result of uplift and subsequent erosion of large parts of the Atlas Rift, rather than subsidence and non-deposition. The subsequent transgression represented by deposition of the Tarhoucht Member (Jbel Wawrmast Formation) would have finally sealed the palaeorelief inherited from the peneplaned horst-and-graben palaeotopography recorded, in a diachronous way, across the "lower–middle Cambrian" transition. A direct consequence of this succession of events is the erosion and reworking of peneplaned palaeoreliefs. Erosion of older strata was the source of fossils derived from different biozones mixed (or condensed) in the Brèche à Micmacca Member.

A third major syn-rift episode took place throughout the Furongian, responsible of the virtual absence of Furongian strata. This was an interval of generalized uplift (probably related to thermal doming) that led to the lack of sedimentation, except in a reduced area of the Jbel El Graara where the presence of Furongian fossils points to sedimentation (Destombes and Feist 1987). The beginning of contrasted drift patterns would, therefore, be located at the beginning of a generalized drowning of the basin, leading to the

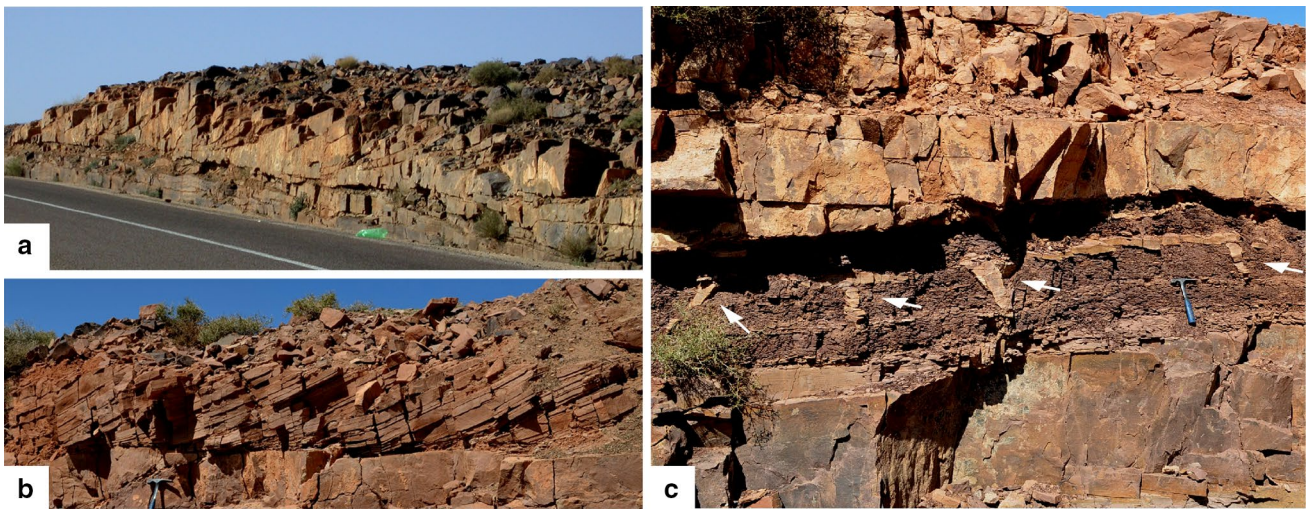

Fig. 10 **a**, **b** Fluvial point-bars of the Tazlaft Member (Asrir Formation) crosscut by the N-140 road at the Jbel Wawrmast stratotype; setting in Fig. 1. **c** Mud cracks infilled with sandstone of the floodplain in which the point-bars of the Tazlaft Member are embedded

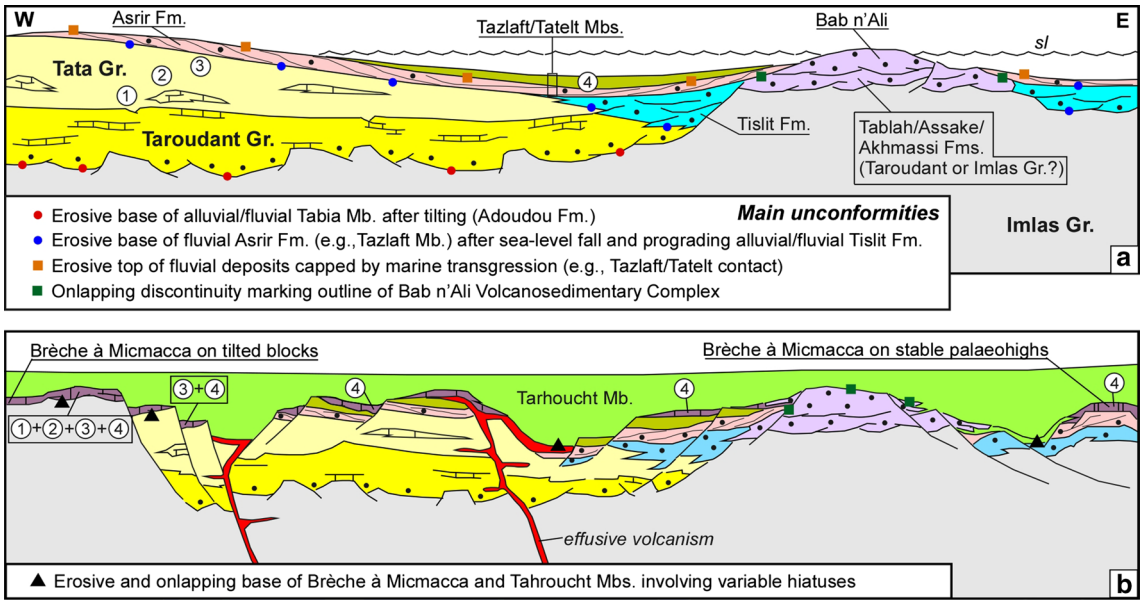

Fig. 11 Tentative palaeogeographical reconstructions of an Ouzellagh-central Anti-Atlas transect from the Atlas Rift reflecting the end of deposition of the Asrir Formation (**a**) and the sealing of a partly peneplaned palaeorelief by the Tarhoucht Member; *1–4 circles* represent successive biozones finally condensed in the Brèche à Micmacca Member; *sl* sea-level

record of the deep, offshore-dominated shales of the Tremadocian Fezouata Formation.

Comparison with neighbouring basins

The Brèche à Micmacca is a distinct marker bed characterized by volcano-bioclastic limestones punctuated by microbial crusts and characterizes hiatal shell accumulations with variable degrees of condensation (even including reworked early Cambrian archaeocyaths; Buggisch et al. 1978; Álvaro et al. 2008a; Álvaro 2014). The rifting pulses that took place across the "lower–middle Cambrian" transition in the Atlas Rift were contemporaneous with a succession of tectonic breakdowns recorded in neighbouring passive-margin basins reported in the Cantabrian Zone, the Iberian Chains (Spain) and the Montagne Noire (France). The "lower–middle Cambrian" boundary is marked by a distinct erosive unconformity, related to tectonic tilting, in the Esla nappe of the Cantabrian Zone (Álvaro et al. 2000) and the southern Montagne Noire (Wotte et al. 2007). Tectonic pulses crossing the "lower–middle Cambrian" boundary were biostratigraphically dated in the Iberian Chains by Álvaro and Vennin (1996) reflecting the propagation of unstable geodynamic conditions throughout the Mediterranean margin of West Gondwana. In the Ossa-Morena Zone of the SW Iberian Peninsula, another latest Ediacaran–Cambrian rift is considered as the lateral prolongation of the Atlas Rift along West Gondwana (Álvaro et al. 2013, 2014b); the "lower–middle Cambrian" transition is represented by the Upper Detrital Group. The latter is characterized by a bimodal magmatism representative of the so-called Main Rift-Related Igneous Event of the whole rift (c. 517–502 Ma; Sánchez-García et al. 2008, 2010) and partly coincides in time with the onset of the volcanosedimentary complexes documented in this paper.

Conclusions

A new stratigraphic architecture is presented in this work linking the Ouzellagh promontory (High Atlas) and the central Anti-Atlas (southern Jbel Saghro) across the "lower–middle Cambrian" transition, based on geometrical relationships of volcanosedimentary complexes and formerly defined lithostratigraphic units. A key stratigraphic marker for this palaeogeographical reconstruction of the Atlas Rift is the unconformity that marks the base of the Brèche à Micmacca Member, which has been known for decades. This was previously interpreted as the result of orogenic, "epeirogenic" and basin reorganization processes. In this work, we interpret this horizon as an onlapping geometry capping the relief of several volcanosedimentary complexes with relic escarpments, which were recorded over a peneplaned horst-and-graben palaeotopography. As a result, the Brèche à Micmacca Member unconformably overlies, in paraconformable to low-angle discordance, a variable basement ranging from the Ediacaran Ouarzazate Supergroup to the Cambrian Asrir Formation. The diachronous volcano-bioclastic limestones of the Brèche à Micmacca represent

lateral migration of extensional tectonics associated with volcanic (tholeiitic) episodes, uplift, tilting, rapid erosion and resedimentation of polymictic clasts. The latter include fossils from different (non-overlapping) biozones and are representative of condensation processes. This stratigraphic framework should be taken into consideration for global chronostratigraphic correlation of the forthcoming (global) Cambrian Series 2/3 boundary.

Acknowledgments The authors thank field support by Nouredine Ait Ayad, Abdelmounim Charif (El Jadida), Xavier Legrain (Lille), Julie Dewit and Robin Honlet (Leuven), and constructive manuscript reviews by Ulf Linnemann and Gregory Walsh. Agreement for using Google Earth images was yielded by Google Brand Permissions. Financial support for this work was provided by project CGL2013–48877 from Spanish MINECO and EU–FEDER.

References

Álvaro JJ (2013) Late Ediacaran syn-rift/post-rift transition and related fault-driven hydrothermal systems in the Anti-Atlas Mountains, Morocco. Basin Res 25:348–360

Álvaro JJ (2014) Rift, pull-apart rift, and continental drift crossword puzzles across the lower–middle Cambrian transition of Iberia and Morocco. GFF 136:2–5

Álvaro JJ, Clausen S (2005) Major geodynamic and sedimentary constraints on the chronostratigraphic correlation of the lower–middle Cambrian transition in the western Mediterranean region. Geosci J 9:145–160

Álvaro JJ, Clausen S (2006) Microbial crusts as indicators of stratigraphic diastems in the Cambrian Micmacca Breccia, Moroccan Atlas. Sediment Geol 185:255–265

Álvaro JJ, Clausen S (2007) Botoman (Lower Cambrian) turbid- and clear-water reefs and associated environments from the High Atlas, Morocco. In: Álvaro JJ, Aretz M, Boulvain F, Munnecke A, Vachard D, Vennin E (eds) Palaeozoic reefs and bioaccumulations: climatic and evolutionary controls. Geol Soc London Spec Publ 275:51–70

Álvaro JJ, Clausen S (2008) Paleoenvironmental significance of Cambrian hiatal shell accumulations in an intracratonic aborted rift, Atlas Mountains, Morocco. In Pratt BR, Holmden C (eds) Dynamics of epeiric seas. Geol Ass Canada Spec Pap 48:39–54

Álvaro JJ, Debrenne F (2010) The Great Atlasian Reef Complex: an early Cambrian subtropical fringing belt that bordered West Gondwana. Palaeogeogr Palaeoclimat Palaeoecol 294:120–132

Álvaro JJ, Subías I (2011) Interplay of phosphogenesis and hydrothermalism in the latest Ediacaran rift of the High Atlas, Morocco. J Afr Earth Sci 59:51–60

Álvaro JJ, Vennin E (1996) Tectonic control on Cambrian sedimentation in south-western Europe. Eclogae Geol Helv 89:935–948

Álvaro JJ, Vennin E (1998) Stratigraphic signature of a terminal Early Cambrian regressive event in the Iberian Peninsula. Can J Earth Sci 35:402–411

Álvaro JJ, Gozalo R, Liñán E, Sdzuy K (1993) The palaeogeography of northern Iberia at the lower–middle Cambrian transition. Bull Soc géol Fr 164:843–850

Álvaro JJ, Vennin E, Moreno-Eiris E, Perejón A, Bechstädt T (2000) Sedimentary patterns across the lower–middle Cambrian transition in the Esla nappe (Cantabrian Mountains, northern Spain). Sediment Geol 137:43–61

Álvaro JJ, Ezzouhairi H, Vennin E, Ribeiro ML, Clausen S, Charif A, Ait-Ayad N, Moreira ME (2006) The Early-Cambrian Boho volcano of the El Graara massif, Morocco: petrology, geodynamic setting and coeval sedimentation. J Afr Earth Sci 44:396–410

Álvaro JJ, Ezzouhairi H, Ait Ayad N, Charif A, Popov L, Ribeiro ML (2008a) Short-term episodes of carbonate productivity in a Cambrian uplifted rift shoulder of the Coastal Meseta, Morocco. Gondwana Res 14:410–428

Álvaro JJ, Macouin M, Ezzouhairi H, Ribeiro ML, Ader M, Charif A., Ait Ayad N (2008b) Late Neoproterozoic carbonate productivity in a rifting context: the Adoudou formation and its associated bimodal volcanism onlapping the western Saghro inlier, Morocco. In: Ennih N, Liégeois JP (eds) The boundaries of the West African Craton. Geol Soc London Spec Publ 297:285–302

Álvaro JJ, Zamora S, Clausen S, Vizcaïno D, Smith AB (2013) The role of abiotic factors in the Cambrian substrate revolution: a review from the benthic community replacements of West Gondwana. Earth Sci Rev 118:69–82

Álvaro JJ, Benziane F, Thomas R, Walsh GJ, Yazidi A (2014a) Neoproterozoic-Cambrian stratigraphic framework of the Anti-Atlas and Ouzellagh promontory (High Atlas), Morocco. J Afr Earth Sci 98:19–33

Álvaro JJ, Bellido F, Gasquet D, Pereira F, Quesada C, Sánchez-García T (2014b) Diachronism of late Neoproterozoic-Cambrian arc-rift transition of North Gondwana: a comparison of Morocco and the Iberian Ossa-Morena Zone. J Afr Earth Sci 98:113–132

Bennett RA, Fay NP, Hreinsdottir S, Chase C, Zandt G (2009) Increasing long-wavelength relief across the southeastern flank of the Sierra Nevada, California. Earth Planet Sci Lett 287:255–264

Bernardin C, Cornée JJ, Corsini M, Mayol S, Muller J, Taychi M (1988) Variations d'épaisseur du Cambrien moyen en Meseta marocaine occidentale: signification géodynamique des données de surface et de subsurface. Can J Earth Sci 25:2104–2117

Bertrand H, Dostal J, Dupuy C (1982) Geochemistry of Early Mesozoic tholeiites from Morocco. Earth Planet Sci Lett 58:225–239

Boudda A, Choubert G, Faure-Muret A (1975) Coupe géologique de l'Ounein. Description lithologique. Réunion sur la limite Précambrien–Cambrien, Agadir-Rabat, Doc A + B

Boudda A, Choubert G, Faure-Muret A (1979) Essai de stratigraphie de la couverture sédimentaire de l'Anti-Atlas: Adoudounien, Cambrien inférieur. Not Mém Serv Géol Maroc 271:1–96

Brögger WC (1879) Om Paradoxidesskifrene ved Krekling. Nyt Mag Natur 24:18–88

Brögger WC (1886) Om aldermen af Olenelluszonen I Nordamerika. Geol Fören Stockholm Förhand 101:182–213

Buggisch W, Heinitz W (1984) Slumpfolds and other early deformations in the early Cambrian of the Western and Central Anti-Atlas (Morocco). Geol Rundsch 73:809–818

Buggisch W, Siegert R (1988) Paleogeography and facies of the "grès terminaux" (uppermost Lower Cambrian, Anti-Atlas/Morocco). In: Jacobshagen VH (ed) The Atlas system of Morocco. Studies on its geodynamic evolution. Lect Not Earth Sci 15:107–121

Buggisch W, Marzela C, Hügel P (1978) Die fazielle und paläogeographische Entiwocklung der infrakambrischen bis ordovizischen Sedimente im Mittleren Antiatlas um Agdz (S-Marokko). Geol Rundsch 68:195–224

Burgess PM, Gurnis M (1995) Mechanisms for the final cratonic stratigraphic sequences. Earth Planet Sci Lett 136:647–663

Burgess PM, Gurnis M, Moresi L (1997) Formation of sequences in the cratonic interior of North America by interaction between mantle, eustatic, and stratigraphic processes. Geol Soc Am Bull 108:1515–1535

Choubert G (1963) Histoire géologique du Précambrien de l'Anti-Atlas. Not Mém Serv Géol Maroc 162:1–352

Corti G (2012) Evolution and characteristics of continental rifting: Analog modeling-inspired view and comparison with examples from the East African Rift System. Tectonophysics 522–523:1–33

Daradich A, Mitrovica JX, Pysklywec RN, Willett SF, Forte A (2003) Mantle flow, dynamic topography, and rift-flank uplift of Arabia. Geology 31:901–904

Dean WT (2005) Trilobites from Çal Tepe Formation (Cambrian), near Seydişehir, Central Taurides, Southwestern Turkey. Turk J Earth Sci 14:1–71

Destombes J, Feist R (1987) Découverte du Cambrien supérieur en Afrique (Anti-Atlas central, Maroc). C R Acad Sci Paris (Sér 2) 304:719–724

Destombes J, Hollard H, Willefert S (1985) Lower Palaeozoic rocks of Morocco. In: Holland CH (ed) Lower Palaeozoic rocks of the world. Lower Palaeozoic of North-Western and West Central Africa, vol. 4. Wiley, Chichester, pp. 57–184

Ellam RM (1992) Lithospheric thickness as a control on basalt geochemistry. Geology 20:53–156

Ezzouhairi H, Ribeiro ML, Ait Ayad N, Moreira ME, Charif A, Ramos JMF, de Oliveira DPS, Coke C (2008) The magmatic evolution at the Moroccan outboard of the West African craton between the Late Neoproterozoic and the early Palaeozoic. In Ennih N, Liégeois JP (eds), The boundaries of the West African Craton. Geol Soc London Spec Publ 297:329–343

Fergusson CL, Offler R, Green TJ (2009) Late Neoproterozoic passive margin of East Gondwana: geochemical constraints from the Anakie Inlier, central Queensland, Australia. Precambr Res 168:301–312

Fitton JG, Saunders AD, Norry MJ, Hardarson BS, Taylor RN (1997) Thermal and chemical structure of the Iceland plume. Earth Planet Sci Lett 153:197–208

Gasquet D, Levresse G, Cheilletz A, Azizi-Samir HR, Mouttaqui A (2005) Contribution to a geodynamic reconstruction of the Anti-Atlas (Morocco) during Pan-African times with the emphasis on inversion tectonics and metallogenic activity at the Precambrian/Cambrian boundary. Precambr Res 140:157–182

Geyer G (1990) Proposal of formal lithostratigraphical units for the Terminal Proterozoic to early Middle Cambrian of southern Morocco. Newsl Stratigr 22:87–109

Geyer G, Landing E (eds) (1995) Morocco'95. The lower–middle Cambrian standard of Gondwana. Beringeria Spec Iss 2:1–171

Geyer G, Landing E (2004) A unified lower–middle Cambrian chronostratigraphy for West Gondwana. Acta Geol Pol 54:179–218

Geyer G, Vincent T (2014) The *Paradoxides* puzzle resolved: the appearance of the oldest paradoxidines and its bearing on the Cambrian Series 3 lower boundary. Paläontol Zeits. doi:10.1007/s12542-014-0225-5

Gilbert GK (1890) Lake Bonneville. US Geol Surv Monogr 1:1–438

Gradstein FM, Ogg JG, Schmitz MD, Ogg GM (eds) (2012) The geologic time scale. Elsevier Amsterdam, p 144

Gurnis M (1988) Large-scale mantle convection and the aggregation and dispersal of supercontinents. Nature 332:695–699

Gurnis M (1990) Bounds on global dynamic topography from Phanerozoic flooding of continental platforms. Nature 344:754–756

Hawkins MP, Beddoe-Stephens B, Gillespie MR, Loughlin S, Barron HF, Barnes RP, Powell JH, Waters CN, Williams M (2001) Carte géologique du Maroc au 1/50 000, feuille Tiwit. Not Mém Serv Géol Maroc 404

Hefferan K, Soulaimani A, Samson SD, Admou H, Inglis J, Saquaque A, Latifa C, Heywood N (2014) A reconsideration of the Pan-African orogenic cycle in the Anti-Atlas Mountains, Morocco. J Afr Earth Sci 98:34–66

Hindermeyer J, Gauthier H, Destombes J, Choubert G, Faure-Muret A (1977) Carte géologique du Maroc: Jbel Saghro-Dadès (Haut Atlas central, sillon sud-atlasique et Anti-Atlas oriental). Echelle 1/200 000. Not Mém Serv Géol Maroc 161

Holm PE (1985) The geochemical fingerprints of different tectonomagmatic environments using hygromagmatophile element abundances of tholeiitic basalts and basaltic andesites. Chem Geol 51:303–323

Hupé P (1953) Contribution à l'étude du Cambrien inférieur et du Précambrien III de l'Anti-Atlas marocain. Not Mém Serv Géol Maroc 103:1–402

Hupé P (1955) Indices d'une phase tectonique salaïrienne dans l'Anti-Atlas marocain. C R Acad Sci Paris 241:971–973

Hupé P (1960) Sur le Cambrien inférieur du Maroc. Rep 21st Int Geol Congr Norden 8:75–85

Irvine TN, Baragar WRA (1971) A guide to the chemical classification of the common volcanic rocks. Can J Earth Sci 8:523–548

Landing E, Geyer G (2007) Reply to Discussion of Liñán et al. on: "Distinguishing eustatic and epeirogenic controls on lower–middle Cambrian boundary successions in West Gondwana (Morocco and Iberia)", by Ed Landing, Gerd Geyer, and Wolfram Heldmaier, published in Sedimentology (2006), 53(4):899–918. Sedimentology. doi:10.1111/j.1365-3091.2007.00930.x

Landing E, Geyer G, Heldmaier W (2006) Distinguishing eustatic and epeirogenic controls on lower–middle Cambrian boundary successions in West Gondwana (Morocco and Iberia). Sedimentology 53:899–911

Liñán E, Perejón A, Sdzuy K (1993) The lower–middle Cambrian stages and stratotypes from the Iberian Peninsula: a revision. Geol Mag 130:817–833

Loi A, Pillola GL, Leone F (1995) The Cambrian and Early Ordovician of south-western Sardinia. Rend Semin Fac Sci Univ Cagliari 65:63–81

Marsh J (1987) Basalt geochemistry and tectonic discrimination within continental flood basalt provinces. J Volcan Geotherm Res 32:35–49

Martins-Neto MA, Catuneanu O (2010) Rift sequence stratigraphy. Mar Petrol Geol 27:247–253

McClay KR, Nichols GJ, Khalil DM, Darwish M, Bosworth W (1998) Extensional tectonics and sedimentation, eastern Gulf of Suez, Egypt. In Purser BH, Bosence DWJ (eds) Sedimentation and tectonics of rift basins. Red Sea, Gulf of Aden. Chapman and Hall, London, pp 223–238

Miall AD (2000) Principles of sedimentary basin analysis. Springer, Berlin

Michard A (1976) Eléments de Géologie Marocaine. Not Mém Serv Géol Maroc 252:1–369

Moussu R (1959) Géologie et gîtes minéraux de la région de l'Ouneïn (Haut Atlas). Not Mém Serv Géol Maroc 145:1–118

O'Connor EA (ed) (2010) Geology of the Drâa, Kerdous, and Boumalne Districts, Anti-Atlas, Morocco. British Geol Surv, Tech Rep IR/10/072:1–310

Olsen KH, Morgan P (2006) Continental rifts: evolution, structure, tectonics. Dev Geotect 25:3–26

Pearce JA (2008) Geochemical fingerprinting of oceanic basalts with applications to ophiolite classification and the search for Archean oceanic crust. Lithos 100:14–48

Pearce JA, Gale GH (1977) Identification of ore-deposition environment from trace element geochemistry of associated igneous host rocks. In Fyfe WS (ed) Volcanic processes in ore deposits. Geol Soc London Spec Publ 7:14–24

Pearce JA, Norry MJ (1979) Petrogenetic implications of Ti, Zr, Y, and Nb variations in volcanic rocks. Contr Miner Petrol 69:33–47

Pouclet A, Aarab A, Fekkak A, Benharref M (2007) Geodynamic evolution of the northwestern Paleo-Gondwanan margin in the Moroccan Atlas at the Precambrian–Cambrian boundary. In Linnemann U, Nance RD, Kraft P, Zulauf G (eds) The evolution of the Rheic Ocean: from Avalonian–Cadomian Active Margin to Alleghenian–Variscan collision. Geol Soc Am Spec Pap 423:27–60

Rooney TO (2010) Geochemical evidence of lithospheric thinning in the southern Main Ethiopian Rift. Lithos 117:33–48

Saleeby J, Saleeby Z, Le Pourhiet L (2013) Epeirogenic transients related to mantle lithosphere removal in the southern Sierra

Nevada region, California: part II. Implications of rock uplift and basin subsidence relations. Geosphere 9:394–425

Sánchez-García T, Quesada C, Bellido F, Dunning G, González de Tanago J (2008) Two-step magma flooding of the upper crust during rifting: the Early Paleozoic of the Ossa-Morena zone (SW Iberia). Tectonophysics 461:72–90

Sánchez-García T, Bellido F, Pereira MF, Chichorro M, Quesada C, Pin C, Silva JB (2010) Rift-related volcanism predating the birth of the Rheic Ocean (Ossa-Morena zone, SW Iberia). Gondwana Res 17:392–407

Sdzuy K (1972) Das Kambrium der Acadobaltischen Faunenprovinz—Gegenwärtiger Kenntnisstand und Probleme. Z Geol Paläont 1972(2):1–91

Sdzuy K (1995) Acerca del conocimiento actual del Sistema Cámbrico y del límite Cámbrico Inferior–Medio. In Gámez JA, Liñán E (eds), Memorias de las IV Jornadas Aragonesas de Paleontología. Institución "Fernando el Católico", Zaragoza, 253–263

Soulaimani A, Bouabdelli M, Piqué AL (2003) L'extension continentale au Néo–protérozoïque supérieur–Cambrien inférieur dans l'Anti-Atlas (Maroc). Bull Soc géol Fr 174:83–92

Soulaimani A, Michard A, Baidder L, Ouanaimi H, Raddi Y (2014) Late Ediacaran–Cambrian structures and their reactivation during the Variscan and Alpine cycles in the Anti-Atlas (Morocco). J Afr Earth Sci 98:94–112

Sun SS, McDounough WH (1989) Chemical and isotopic systematic of oceanic basalts: implications for mantle composition and processes. In Saunders AD, Norry MJ (eds), Magmatism in the ocean basins. Geol Soc London Spec Publ 42:313–345

Walsh GJ, Yazidi A, Benziane F, Burton WC, El Fahssi A, Stone BD, Yazidi M, Saadane A, Aleinikoff JN, Ejjaouani H, Kalai M (2008) Carte géologique au 1/50 000. Feuille Timdghas, Not Mém Serv Géol Maroc 471

Walsh GJ, Benziane F, Aleinikoff JN, Harrison RW, Yazidi A, Burton WC, Quick JE, Saadane A (2012) Neoproterozoic tectonic evolution of the Jebel Saghro and Bou Azzer-El Graara inliers, eastern and central Anti-Atlas, Morocco. Precambr Res 216–219:23–62

Wilson M (1994) Igneous petrogenesis: a global tectonic approach. Harper Collins, London

Winchester JA, Floyd PA (1976) Geochemical magma type discrimination; application to altered and metamorphosed basic igneous rocks. Earth Planet Sci Lett 28:459–469

Winchester JA, Floyd PA (1977) Geochemical discrimination of different magma series and their differentiation products using immobile elements. Chem Geol 20:325–343

Wotte T, Álvaro JJ, Shields GA, Brasier M, Veizer J (2007) C–, O– and Sr–isotope stratigraphy across the lower–middle Cambrian transition of the Cantabrian Mountains (Spain) and the Montagne Noire (France), West Gondwana. Palaeogeogr, Palaeoclimat, Palaeoecol 256:47–70

Zhou J, Wang X, Qiu J, Gao J (2004) Geochemistry of Meso- and Neoproterozoic mafic ultramafic rocks from northern Guangxi, China: arc or plume magmatism? Geochem J 38:139–152

Żylińska A, Masiak M (2007) Cambrian trilobites from Brzechów, Holy Cross Mountains (Poland) and their significance in stratigraphic correlation and biogeographic reconstructions. Geol Mag 164:661–686